8-2002

Platinum/silica Thin Films by Chemical Vapor Deposition

Tyler Philip Martin

PLATINUM/SILICA THIN FILMS BY CHEMICAL VAPOR DEPOSITION

By

Tyler Philip Martin

B.S. University of Maine, 2000

A THESIS

Submitted in Partial Fulfillment of the

Requirements for the Degree of

Master of Science

(in Chemical Engineering)

The Graduate School

The University of Maine

August, 2002

Advisory Committee:

William DeSisto, Assistant Professor of Chemical Engineering,

David Neivandt, Assistant Professor of Chemical Engineering

Carl Tripp, Associate Professor of Chemistry

PLATINUM/SILICA THIN FILMS BY CHEMICAL VAPOR DEPOSITION

By Tyler Philip Martin

Thesis Advisor: Dr. William DeSisto

An Abstract of the Thesis Presented
in Partial Fulfillment of the Requirements for the
Degree of Master of Science
(in Chemical Engineering)
August, 2002

Composite thin films consisting of platinum and silica $(SiO)_2$ have been fabricated by chemical vapor deposition (CVD). These films were studied for possible future use in enhancing the selectivity of sensors for the chemical warfare agent sarin. Chemical vapor deposition is a thin film growth technique in which precursor molecules are carried into a reactor and decomposed, often at high temperature, to produce a thin solid film. A new cold wall CVD reactor was built for this work. The platinum precursor used in this work was platinum acetylacetonate $[Pt(acac)_2]$ and the silica precursor was tetraethoxysilane (TEOS). It was found that by simultaneously decomposing the two together, the decomposition temperature of TEOS was lowered from an expected 973K to as low as 593K. In addition, the composition of the films was found to be self limiting at one silicon atom per platinum atom over a wide range of deposition conditions and growth rates. X-ray diffraction (XRD) and x-ray photoelectron spectroscopy (XPS) were used to characterize the films.

An *in situ* fourier transform infrared spectroscopy (FTIR) study was undertaken to gain further insight into this phenomena. The equipment had to be significantly modified to combine the CVD system with the spectrometer. Striking spectral evidence for the decomposition of TEOS at low temperatures is presented. A reaction is proposed based on the results of this work and the work of others.

This work has implications for the use of catalysis in CVD to reduce the deposition temperature. A lower deposition temperature is desirable because a wider range of substrates can be used and it results in less film stress upon cooling. There are also implications for the production of composite films by CVD and the use of *in situ* FTIR spectroscopy for studying CVD systems.

ACKNOWLEDGEMENTS

I would like to acknowledge the contributions of several people that have made this an extremely rewarding and valuable experience. First and foremost, I would like to thank my advisor Dr. Bill DeSisto for his constant encouragement and excellent instruction in the methodologies of research. The members of my thesis committee, Dr. Carl Tripp and Dr. David Neivandt, provided valuable suggestions and assistance, particularly with the FTIR portion of the thesis.

Dan Jolicoeur provided invaluable technical assistance in designing and fabricating key components of the equipment. Amos Cline showed me the basics of wiring and helped in troubleshooting electrical problems in the equipment.

Sofian Kanan was extremely helpful over all aspects of the FTIR study, from initial assistance with the equipment, with which I was unfamiliar, to analysis of the data.

George Bernhardt was extremely helpful in the compositional analysis of the composite films as well as showing me the growth rate determining procedure. Luke Doucette, Scott Moulzolf, and Mike Call also provided assistance with the XPS and XRD equipment.

This work was supported by the Office of Naval Research through Grant # N 00014-01-1-0921.

I would like to thank the other graduate students in the program for their friendship and all the good times. Finally, I would like to thank my fiancée, Andrea Page, for all her support, encouragement and love, without which I probably would not have undertaken these studies.

TABLE OF CONTENTS

LIST OF TABLES

LIST OF FIGURES

INTRODUCTION

Semi-conducting metal oxide (SMO) materials have been studied for use as sensors. These materials include WO_3, SnO_2, and others. While extremely sensitive to reducing gases, problems arise because they detect a wide range of gases, and therefore are not selective to the specific gas of interest. Work is being done with the goal of making these sensors selective to a specific target gas.

Sarin is of interest because it is a well known nerve agent that has been previously used in terrorist attacks in Japan. A cult carried out two terrorist attacks in Japan using Sarin nerve gas. The first was in Matsumoto, seven people were killed and 56 hospitalized. The second was carried out in the Tokyo subway system by attackers puncturing aerosol cans containing sarin and a dispersant. This attack killed 12 people and injured 5500, with some left with permanent damage. Its use is also suspected by Saddam Hussein against Kurds in his own country, Iraq. Effective countermeasures exist that can greatly mitigate the damage if they can be administered rapidly, but if used in error, can cause great damage. Therefore, a highly accurate, rapid detection system is required.

The ultimate goal of work in this area is a compact sensor unit capable of detecting multiple chemical and biological agents. This unit should be small enough to be worn on soldiers' uniforms when going into battle so that they will know if these agents have been deployed and can take protective measures. This unit could also be used by emergency response personnel responding to the site of a possible terrorist attack. If they had this capability, they could administer countermeasures to casualties on site and take appropriate precautions to avoid becoming ill themselves.

The current level of technology is some way from achieving this goal. A working prototype capable of quickly detecting many possible chemical and biological agents has been made at Oak Ridge National Laboratory. It works on principles of mass spectroscopy, which is a very different way of attacking the problem than SMO sensors. The unit weighs approximately 170 lbs., which means, of course, that each soldier could not carry one into battle. It costs $200, 000, which is prohibitive for use by civilian departments. The advantage of using SMO sensors, if they can be made selective enough, is that they can be very small, near 5 mm square, and cheaply.

The goal of this work was to study the chemical vapor deposition (CVD) of thin films that could be deposited on top of SMO sensors to aid in the selective detection of the chemical warfare nerve agent sarin. In pursuit of this goal, composite thin films of platinum and silica (SiO_2) have been fabricated by chemical vapor deposition. The platinum precursor was platinum acetylacetonate ($Pt(acac)_2$) and the silica precursor was tetraethylorthosilicate (TEOS), with oxygen added as a co-reactant. It was found in the course of this work that the decomposition temperature of TEOS was lowered from approximately 923K to as low as 573K by depositing it simultaneously with $Pt(acac)_2$. Also, the amount of silica incorporated into the film was limited, so that the maximum Si/Pt ratio was 1.0 under all conditions studied.

This work has advanced knowledge in the area of deposition of composite films by chemical vapor deposition and in lowering the decomposition temperature through catalytic-like reactions of deposition precursors. Also, this work has implications for *in situ* FTIR studies of CVD systems.

BACKGROUND

Chemical Vapor Deposition

Chemical vapor deposition is a widely used technique for thin film formation. Originally used for refining metals in the 1800's, it is now best known in the semiconductor industry, where it has been used since the 1960's. Single crystals of the base semiconductor material silicon can be deposited by CVD of dichlorosilane [1]. Subsequent metallic, insulating and dielectric layers can be deposited by various CVD techniques, such as metal-organic CVD (MOCVD) and plasma-enhanced CVD (PECVD). It has also gained use in the coating industry, for wear-resistant or corrosion resistant coatings, the solar energy industry, high temperature superconductor research, as well as many other areas.

General Process and Equipment of CVD

The overall process of CVD involves transporting precursors into a reactor. There, they adsorb on the surface of a substrate, and then decompose, usually at moderate to high temperatures, to leave behind a film. The precursors can also undergo gas phase reactions prior to adsorbing onto the substrate. Ideally, the by-products of reaction then

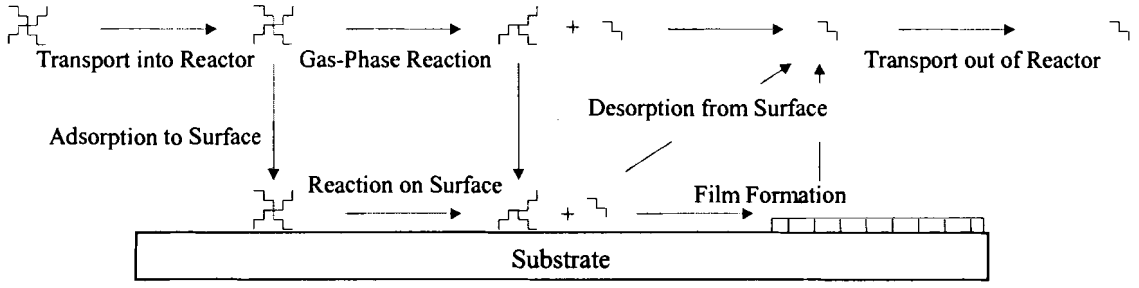

Figure 1. Schematic of Chemical Vapor Deposition

desorb off the surface and are transported out of the reactor. In reality, the by-products can be incorporated into the film as impurities. A schematic of this is shown in Figure 1. Co-reactant gases can also be fed to the reactor to enhance the film deposition. For example, co-reactant gasses can reduce the deposition temperature.

The precursors can be gaseous, liquid, or solid at room temperature. They usually involve a central atom with surrounding ligands. These ligands can range from hydrogen (hydrides) to halogens (halides) to bulky organic ligands. Gaseous precursors can be metered directly into the reactor. A common bubbler-style delivery system for liquid precursors is shown in Figure 2. The inert carrier gas is bubbled through the liquid, becoming saturated with precursor before being fed to the reactor. The same delivery system can be used for solid precursors, but it is desirable to use gaseous or liquid precursors instead of solid. Often, solid precursors must be heated to have a reasonable vapor pressure. This leads to the major disadvantage that, with time, solid precursors send less vapor into the reactor [2], which is due mainly to sintering of the powder, so that there is less surface area of powder. This reduces the rate of diffusion of precursor vapor from the bulk powder into the carrier gas stream, making repeatability difficult to attain. The reduced delivery rate can also be due to decomposition in the bubbler. Various solid

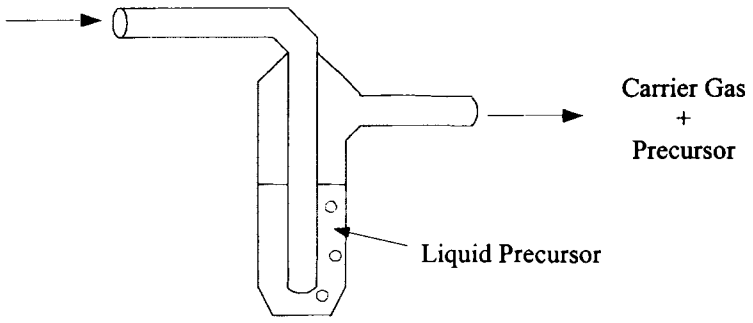

Figure 2. Bubbler for delivery of liquid precursor

precursor delivery schemes have been developed to attempt to mitigate this problem [3,4], but these will not be discussed here.

If the vapor pressure of the precursor is known, the flow rate of precursor into the reactor can be determined by

$$F_{Precursor} = F_{Carrier\ Gas}\ (P_{Precursor}/P_{Bubbler}) \qquad (1)$$

where $F_{Precursor}$ is the flow rate of precursor into the reactor, $F_{Carrier\ Gas}$ is the flow rate of carrier gas through the precursor source bubbler, $P_{Precursor}$ is the vapor pressure of the precursor at the vaporization temperature, and $P_{Bubbler}$ is the total pressure in the precursor source bubbler, which includes the carrier gas pressure and the precursor pressure. The use of this equation requires a key assumption; that the carrier gas is saturated with precursor. While this is a valid assumption for liquid precursors, it breaks down for solid precursor, where the carrier gas is not likely to be saturated. This is another major difficulty with the use of solid precursors.

Advantages and Disadvantages of CVD

Chemical vapor deposition has several advantages over other thin film deposition techniques. The equipment is significantly simpler to operate and maintain, leading to significant cost savings. For instance, it does not require a high or ultra-high vacuum system, as in the physical vapor deposition (PVD) techniques sputtering or evaporation. Less energy is required for CVD compared to these PVD techniques. The formed film is conformal, i.e. it matches the shape of the substrate. The PVD techniques above result in of line-of-site deposition, in which, for instance, the bottom of trenches may not have the same thickness of deposited film as the substrate surface. Much better control of film properties, such as thickness, can be achieved than with liquid phase deposition

techniques, such as spin-on coating. It can also be difficult to remove all the solvent when performing spin-on coating. The large use of solvent necessary for spin-on coating also makes the process an environmental concern if the solvent is not aqueous.

The major disadvantage of CVD is contamination of the film by incomplete decomposition of the precursors, so that some ligand material becomes incorporated into the film. The formed film can have hydrogen, halogen, or carbon and oxygen impurities, which can adversely affect the performance of the film. Although the processing temperatures are reduced when compared to evaporation or sputtering, the temperatures can still be too high to use on the desired substrate. The addition of ozone or reaction in plasma can lower the deposition temperature, but these conditions can also be too harsh for certain substrates. Some new CVD techniques[5], not discussed here, have avoided this limitation. There can also be problems with the precursor decomposing in the gas phase, producing fine particles that can ruin the film (known as gas phase nucleation).

Chemical vapor deposition is limited by the availability of precursors for the desired film. There must be a precursor molecule that is sufficiently volatile, and the precursor must be stable over time so that the amount of material going into the reactor is stable with time. Once in the reactor, the precursor must decompose at a reasonable temperature, but only upon adsorption to the substrate surface. Some gas phase decomposition often takes place, but the primary decomposition must be on the substrate surface. So, the reaction must be slow enough so that the precursor doesn't rapidly decompose in the gas phase, causing gas phase nucleation, but fast enough so that it has a high yield, i.e., most of the precursor reacts to form a film. The decomposition must be clean, so that the ligands are not incorporated into the film. For example, in metal-

organic CVD, the ligands should be designed so that the bond between the metal and the ligand is weaker than the internal ligand bonds, so that the metal-ligand bond breaks first. The by-products of the decomposition must be volatile so that they can be transported out of the reactor. Finally, safety and corrosion have to be a consideration. Hazardous precursors, or hazardous and/or corrosive by-products, greatly increase the cost and complexity of a reactor system and should be avoided.

CVD of Silica Films

Pyrolysis of Tetraethoxysilane

The chemical vapor deposition of silica (SiO_2) is an important process in the microelectronics industry and has been widely studied. Silica is an insulator with a good dielectric strength of 6-7 MV/cm and dielectric constant of 3.9-4.2 [1]. Silica was originally deposited by CVD using silane (SiH_4) and oxygen. The deposition temperature was near 673K. This process had a high growth rate, but film quality problems arose due to gas phase nucleation. Tetraethoxysilane (TEOS), also known as tetraethylorthosilicate, was found to form more suitable films when thermally deposited at 973K under low pressure. The vapor pressure parameters of TEOS for the Antoine equation

$$\mathrm{Log}_{10} P = A - (B/(T+C)) \qquad (2)$$

have been determined where P is in bar, A = 4.17312, B = 1561.277, and C = -67.572. The pyrolysis of TEOS to form silica has been thoroughly studied [6-19].

Huppertz and Engl [6] reported on modeling of the deposition of silica from TEOS at reduced pressures (1-3.75 Torr) in 1979. They found the growth was kinetically limited from 940K to 1000K, and diffusion limited above 1000K.

Adams and Capio [7] reported on the reduced pressure (0.2-0.3 Torr total pressure) deposition of silica and phosphorous-doped silica in 1979 at 923K-1073K. They found that the pure silica films had a thickness uniformity of ±1% below 1048K over a large reactor, and that the films were conformal with a low defect density. The phosphorous doped films were found to have less thickness uniformity.

Levin and Evans-Lutterodt [8] studied the step coverage of several silica precursors for doped and undoped films. Step coverage is a measure of how well the deposited film covers trench walls and bottom. They studied deposition at 923K-1053K and found that the undoped film formed from TEOS had the best step coverage, and that the step coverage was independent of deposition temperature.

Vogel et al. [9] examined the effect of the deposition atmosphere on the electrical properties of the film. The deposition was carried out at 973K on silicon substrates. They found that the use of oxygen as a carrier gas greatly improved both the bulk oxide and the substrate-bulk interface, but also reduced deposition rates by approximately 30%. This indicates that oxygen plays a role in the decomposition of TEOS.

Becker et el. [10] studied the deposition of silica from TEOS below 1 Torr total pressure and at 923K-1073K. They found that thickness variation was less than 5% if the deposition temperature was below 1003K, and increasing the deposition temperature to 1053K increased the thickness variation to 25%. Also, they found that the rate-limiting mechanism changed from reaction controlled to diffusion controlled above 973K. An increase in total pressure resulted in better step coverage, but higher film thickness variation. Finally, they also deposited TEOS using oxygen carrier gas, and found no significant differences in the electrical properties of the films from those deposited in an

inert atmosphere. No data on film growth characteristics (rate, thickness variation) are provided for the oxygen experiments.

Morancho et al. [11] investigated the decomposition of TEOS using downstream (post reactor) gas chromatography. They studied the temperature range of 773K-1073K. Decomposition began as low as 793K, but full pyrolysis did not occur until 953K. No unreacted TEOS remained above approximately 1023K. The main by products of reaction were ethylene and ethanol, with ethanal being formed in small quantities.

Desu [12] examined the decomposition chemistry of TEOS in detail. Through gas chromatography and FTIR analysis of by-products caught by a liquid nitrogen trap, he found that the major products of decomposition are ethanal, ethylene, ethanol, and ethane when reacted at 973K. Desu determined that the key rate-limiting step is the gas-phase formation of an intermediate, which was proposed to occur through a free radical mechanism. Since the decomposition is initiated by a free radical mechanism, he proposes that the presence of radicals more stable than those formed by TEOS decomposition should reduce the activation energy of decomposition, i. e. catalyze the reaction. Assuming a free radical mechanism, the ethyl ($\cdot C_2H_5$) radical would be formed in the initiation step, so radicals more stable than this should catalyze the reaction. The stability of the radical increases with increasing delocalization of the radical, so secondary or tertiary hydrocarbon radicals are more stable than the ethyl radical, and the acetoxy radical, for example, is even more stable.

Desu and Kalindini [13] continued his work by modeling the low pressure CVD deposition of silica from TEOS using a finite element method, taking into account both homogenous (gas-phase) and heterogeneous (surface) reactions. They were able to

successfully model growth at varying deposition temperature, TEOS partial pressure, and position in a 30 cm reaction zone. They were also able to show that a lumped equation model, combining both homogeneous and heterogeneous reactions, did not agree with the data.

Later, Desu and Senkevich [16] showed that the proposal of an initial gas phase decomposition was correct by first decomposing TEOS in a pyrolysis chamber at 953K, then bringing the products into a deposition chamber where a film was formed at 339K. A long-lived intermediate is formed that is carried into the deposition chamber, where it adsorbs on a substrate and decomposes. They did not determine the intermediate species.

Sorita et el. [14] also examined the mechanism and step coverage of deposition. By examining the data from a specialized experimental method, they determined that there were likely two gas-phase intermediates formed, one of which is a high activity specie with a sticking probability near 1.0 and the other a low activity specie. They proposed that a dimerization reaction was taking place to form the low activity intermediate.

Kim and Gill [15] examined the LPCVD of silica from several precursors, and found that TEOS provided the highest deposition rate. Their studies were carried out in a cold wall reactor with *in situ* growth rate measurement. They propose that, in a cold wall reactor, the reaction occurs through dissociative adsorption of TEOS, and suggest that the formation of gas phase intermediates is only important in hot-wall reactors. A cold wall reactor has walls that are not hot enough to cause the decomposition of the precursor, whereas in a hot wall reactor, the walls are held at the deposition temperature.

Recent modeling of TEOS deposition has been carried out by Coltrin et al. [19]. The gas phase reactions they used for their model are given in Table 1, along with the

Arrhennius constants for the reaction. The initial TEOS decomposition step is assumed to be a four-centered β-hydride elimination, resulting in triethoxysilanol [$Si(OH)(OC_2H_5)_3$] and ethylene (reaction 1). Other reactions are of course possible, but the authors decided that they play only very minor roles, so they were left out in the interest of simplicity. The surface reactions (not shown here) the authors include show the absorption of TEOS and triethoxysilanol only, followed by the elimination of the organic ligands. The other specie in Table 1, the dimer, is not shown to absorb in their model, indicating that the initial decomposition to form triethoxysilanol is the key step.

Table 1. Gas-phase reactions in TEOS CVD (From Coltrin et al. [19])

Reaction No.	Reaction	A^a	E_a (cal/mole)
1	$Si(OC_2H_5)_4 \leftrightarrow Si(OH)(OC_2H_5)_3 + C_2H_4$	4.9×10^{13}	61460
2	$Si(OC_2H_5)_4 + H_2O \leftrightarrow Si(OH)(OC_2H_5)_3 + C_2H_5OH$	1.0×10^{11}	25000
3	$Si(OH)(OC_2H_5)_3 + Si(OC_2H_5)_4 \leftrightarrow O(Si(OC_2H_5)_3)_2 + C_2H_5OH$	1.0×10^{11}	30000
4	$2\ Si(OH)(OC_2H_5)_3 \leftrightarrow O(Si(OC_2H_5)_3)_2 + H_2O$	1.0×10^{11}	30000

a Units vary by reaction order, but are expressed in moles, cm, and s.

Other recent modeling studies include those by Labun et al. [18] and Merchant et al. [17]. They study problems with feature (micro) scale modeling, and integration of feature scale with reactor (macro) scale modeling.

Fourier Transform Infrared Spectroscopy (FTIR) studies of TEOS decomposition will be described later

Other CVD Systems Using Tetraethoxysilane

The high temperature required for pyrolysis of TEOS is a major disadvantage of that process. The silica films formed from TEOS were very good, however, so other deposition techniques using TEOS were developed to overcome this obstacle. These are the use of ozone as a co-reactant at atmospheric pressure (APCVD), and the use of a plasma system, known as plasma-enhanced CVD (PECVD). Ozone addition results in the reduction of the deposition temperature to 673K and results in good quality silica films. First proposed in the 1980's, this system has become widely used in industry for the manufacture of very large scale integrated (VLSI) circuits [1].

Nguyen et al. [20] studied both the ozone/TEOS APCVD system and the PECVD system. Ozone was added at ~15% in an oxygen stream. For the ozone/TEOS system, they found that increasing the deposition temperature up to 673K increased the growth rate, but temperatures higher than this resulted in a slight decrease in growth rate. They attributed this to the change from the kinetically controlled regime to the diffusion controlled regime at this temperature and the increased elimination of hydrogen from the bulk film at higher temperatures. This increased elimination of hydrogen results in a higher quality film. Deposition occurred as low as at 473K, but the films were of low quality and the growth rate was very slow at this temperature. The addition of a glow-discharge plasma (still adding ozone and oxygen) resulted in faster growth rates and films with less hydrogen at lower temperatures. Films deposited at 573K using a plasma had less hydrogen than those deposited at 713K in the ozone system. Films formed using a plasma, however, were less conformal than those formed with ozone. This indicates that

the plasma enhances reactivity at the surface to the point where the surface migration of reactive species was decreased.

Kubo et al. [21] used a technique involving both plasma and ozone CVD to form void-free films for VLSI applications. They used a dual-frequency plasma to first deposit an underlayer of silica on top of aluminum wiring schemes, then deposited the bulk of the film using ozone/TEOS APCVD.

Other precursors for the deposition of silica have also been developed, but these will not be treated here, except to describe a paper in which diethylsilane (DES) was used, because the results are relevant to this thesis. Hochberg et al [22] described the deposition of silica from DES and oxygen, and examined the affect of various additives, such as ethene, helium, toluene, methylchloride and various peroxides. DES normally is deposited near 673K with oxygen to form silica films. The authors found that ethene and helium had little affect on the deposition process. Toluene and methylchloride inhibited the growth rate, which they believed was due to the free radical scavenging nature of these species. The peroxides, which acted as source molecules for free radicals, resulted in a reduction of the growth temperature to as low as 523K with the addition of $(t\text{-}BuO)_2$. This is similar to the deposition temperature reduction observed in this work, and the affect of free radicals proposed by Desu [12]. Film quality and step coverage was comparable to pure DES/O_2 deposition.

CVD of Platinum Films

Platinum thin films have many uses, including electrodes, catalysts, and protective and decorative coatings. Particularly, the use of platinum for electrodes in

memory storage applications is being explored because of platinum's excellent corrosion resistance and high temperature stability.

Deposition from Platinum(II) Aceteylacetonate

Platinum(II) acetylacetonate is commonly used as a precursor for platinum thin film deposition because it is volatile, stable, and commercially available. Its structure is

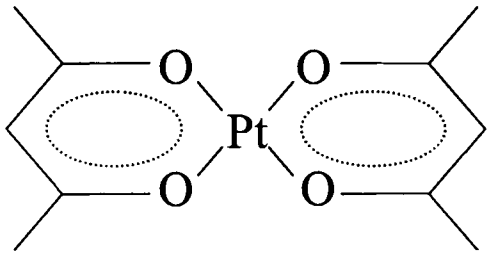

Figure 3. Structure of $Pt(acac)_2$

shown in Figure 3. It is a yellow solid at room temperature, and must be heated to achieve a vapor pressure sufficient for delivery into the reactor. Rand [23] first evaluated $Pt(acac)_2$ as a precursor for platinum thin film deposition at reduced pressure. He found it was unsuitable because the films were contaminated with approximately 50 atomic% carbon when deposited at 773-873K in an inert atmosphere.

Goto and colleagues [24,25] found that the addition of oxygen to the growth atmosphere resulted in nearly carbon free platinum films. Without oxygen, they found that the growth is kinetically-controlled below 743K and diffusion controlled above this temperature. The addition of oxygen reduced the growth rate and seemed to result in a linear dependence on temperature in the range 623K-873K, although the data is somewhat scattered. In the range 773K-873K they were able to grow epitaxial films on single crystal sapphire substrates at a total pressure of 2 Torr.

Arndt et al [26] examined the growth kinetics of $Pt(acac)_2$ with and without oxygen over the range 1.9-7.5 Torr. Without oxygen, they found a carbon:platinum ration of 2.4:1 at 723K. They found that the addition of oxygen resulted in a constant deposition rate over 523K-593K, and greatly reduced the carbon contamination of the films, to nearly zero carbon content, as determined by wavelength dispersive spectroscopy.

Kojima et al [27] used CVD of $Pt(acac)_2$ to deposit platinum membranes inside porous alumina for hydrogen separation. The pressure was maintained at 757 Torr outside the membrane and 450 Torr inside the membrane, which is in contrast to the previous studies carried out at low pressure. No oxygen was used, and they deposited at 493K, lower than previous studies, to ensure the $Pt(acac)_2$ was able to diffuse into the pores before decomposing. Deposition continued until the pores were plugged, as measured by nitrogen flux. This shows an alternative use of the CVD process.

Battison et al. [28] studied deposition from $Pt(acac)_2$ in the presence of oxygen over the range 653-693K and 0.6 Torr. They found that the growth rate was independent of deposition temperature above 668K. The deposited films were always polycrystalline, regardless of substrate or deposition temperature.

Fragala et al. [29] found they could deposit Pt(100) oriented films on a non-epitaxial surface, Hastelloy C276. The deposition temperature was explored over the range 473-773K, and the total pressure was 4 Torr, and oxygen was added to between 33-66% of the growth atmosphere. Films grown for 15 min, resulting in films approximately 500 nm thick, showed random polycrystalline orientation, whereas longer growth times resulted in (100) oriented films greater than 1000 nm thick. Deposition temperatures above 723K resulted in randomly oriented films, as did growth in a less than 50% oxygen atmosphere.

Godinez et al [30] studied the deposition from $Pt(acac)_2$ for use as electrodes on yttria stabilized zirconia, both with and without oxygen, at 663-673K and 1 Torr. They found that the addition of oxygen resulted in films with no observable Auger signals of carbon. Also, films grown without oxygen had smaller grain sizes than those grown with oxygen.

Igumenov and colleagues [31-33] have studied the deposition of platinum from $Pt(acac)_2$ for use as coatings on titanium electrodes in the electrodialysis of seawater. The high corrosion resistance of platinum leads to longer lifetimes for the electrodes. They determined the vapor pressure parameters of $Pt(acac)_2$ as this is important for the use of CVD precursors. They carried out experiments using the flow method and the Knudsen method, which allowed extending the range of temperatures that could be studied. They then combined this data with literature data taken using the zero-gauge method. Their final result for the Clausius-Clayperon equation

$$\text{Ln } P = B - A/T \qquad (3)$$

where P is in atm, B = 20.19, and A = 12737 for $Pt(acac)_2$ (P = 8.4 mTorr at 403K). They also characterized four other platinum group metal acetylacetonate compounds. Platinum was deposited at 533-653K in the presence of oxygen, which comprised 6-29% of the growth atmosphere. In general, they found the best corrosion resistance for platinum films grown at the lowest carrier gas flow rate and deposition temperature.

Finally, Carta et al [28] studied deposition from $Pt(acac)_2$ at 693K and 1 Torr, using oxygen, water and hydrogen as co-reactant gases onto quartz and CaF_2 substrates. They found that, no matter the deposition atmosphere, the platinum films contained 16 atomic% C and 4 atomic% O. This was determined using XPS and after 14 min of

sputtering by an Ar^+ beam at 3.0 kV to remove the surface layer, which is likely to be contaminated by atmospheric oxygen and carbon. Secondary ion mass spectroscopy (SIMS) detected the presence of Pt-organic clusters both on the film surface and in the bulk, which is likely due to incomplete precursor decomposition. They attributed the oxygen in the film to the acetylacetonate ligand, which has an XPS O1s signal of 532.0-532.3 eV. The only apparent effect of growth atmosphere was that water resulted in a larger grain size on the quartz substrates. In general, the CaF_2 substrates resulted in a larger average grain size (148 ± 8 nm) than the quartz substrates (123 ± 9 nm).

In a related use of $Pt(acac)_2$, Utrianen et al [34] attempted atomic layer epitaxy (ALE) by alternately pulsing the precursor to saturate the substrate surface, then pulsing H_2 to reduce and remove the acetylacetonate ligand. They found that $Pt(acac)_2$ was unsuitable for ALE because it decomposed pyrolitically, even at the low temperature of 428K. Therefore, the layer by layer deposition desired for ALE could not be achieved.

Other Platinum Precursors

Several other platinum precursors have been created to attempt to avoid some of the problems with using $Pt(acac)_2$. In essence, this involves trying to increase the volatility and to find precursors that are liquid at room temperature, each of which would make precursor delivery easier and more repeatable. It is well known that the delivery of solid precursors is difficult to control[2], as described in the Background section.

Platinum(II) hexaflouroacetylacetonate [35,36], abbreviated $Pt(hfa)_2$ is a closely related, commercially available (Alfa-Aesar, Gelest) compound in which the hydrogen of the acac methyl groups (see Figure 1) are replaced by fluorine atoms. This makes the compound considerably more expensive than $Pt(acac)_2$. Although the precursor is a

solid, this substitution increases the volatility significantly, so that the coefficients for the Clausius-Clayperon equation (Equation 1) are A = 9320K and B = 29.3, where P is in Pascals (P = 560 mTorr at 373K) [35]. Unfortunately, unless hydrogen is used as a co-reactant gas, the deposited films contain fluorine [35], a major disadvantage in this work. Electron impact mass spectroscopy (EI-MS) of $Pt(hfa)_2$ showed that the triflouromethyl groups break off first, that the platinum-oxygen bond is strong, and that one of the two hexflouroacetylacetonate ligands remains intact and bonded to the metal. These results are similar to those found when studying the decomposition of the acetylacetonate ligand in $Mg(acac)_2$ [37]. While caution is advisable in transferring these results to $Pt(acac)_2$, the two sets of results taken together provide some insight into the likely decomposition pathway of the acetylacetonate ligand in $Pt(acac)_2$.

Other platinum precursors for CVD include $Pt(CO)_2Cl_2$ [23], $Pt(PF_3)_4$ [23], $CpPtMe_3$ (where Cp is η^5-C_5H_5) [38], Cp^*PtMe_3 (where Cp^* is η^5-$Ch_3C_5H_4$) [39-41], $PtMe_2(MeNC)_2$ [42], $PtMe_2COD$ and variations (where COD is 1,5-cyclooctadiene) [35,42-44], $Pt(\eta^3\text{-}C_3H_5)(\eta^5\text{-}C_5H_5)$ [42], $[PtMe_3(acac)]_2$ [42], and $Pt(CH_2CH_2CH_2CH{=}CH_2)_2$ [45]. In general, while these precursors are more volatile than $Pt(acac)_2$, they require co-reaction with hydrogen to produce low-carbon films, are air and moisture sensitive, and are not commercially available. These factors combine to make these precursors undesirable for this work and unlikely to be used in industrial processes.

CVD of Composite Films

Chemical vapor deposition is widely used to fabricate films of more than one component. CVD is a useful method for making composite thin films because the

composition and properties of the films can be more easily tailored to specific applications than by other methods. A common example is the use of TEOS with precursors for boron and phosphorous to make borophosphosilicate glass (BPSG). The dopants greatly increase the glass reflow, an important property in microelectronic fabrication [1]. Metal/metal-oxide films [46,47], metal-metal films [32,48], and ceramic composite films [49] have been formed by composite CVD. High temperature superconductors have also been fabricated [50,51]. Usually, composite films are formed from two or more precursors that are co-reacted. However, single-source precursors have also been used to make composite films. Veith et al [47,52] used a nickel-tin organometallic compound to create a biphasic composite film of Ni_3Sn_4/SnO_2, and other single source precursors to make ceramic composites and metals dispersed in a ceramic matrix.

Crichtlow et al. [46] formed composite platinum/tin oxide films for sensing applications from $Pt(acac)_2$ and Tin(IV) t-butoxide ($Sn(OBu^t)_4$) in an inert atmosphere . They found that despite of the lack of oxygen co-reactant, the films contained no carbon, indicating the $Sn(OBu^t)_4$ aided in the decomposition of the acetylacetonate ligands to volatile non-reactive species.

Battison et al. [28,53] co-deposited platinum and TiO_2 from $Pt(acac)_2$ and titanium tetraisopropoxide (TTIP). They found that the growth of the composite film was simply the sum of the growth of the individual components. Therefore, the co-deposition process did not have any effect on the decomposition of the precursors and film formation of the individual components.

The work by Godinez et al [30] described above also involved the deposition of Pt/ZrO_2 films for use as electrodes. They simultaneously decomposed $Pt(acac)_2$ and

$Zr(acac)_2$ with oxygen. There was no apparent change in the growth of either component due to the simultaneous decomposition.

Of the most interest to this work, Gladfelter et al. [49] formed amorphous $Ti_xSi_{1-x}O_2$ films using TEOS and two titania precursors, TTIP and titanium tetranitrate (TN). They found that the use of either of the two titania precursors resulted in the decomposition of TEOS at temperatures as low as 623K. When using TTIP the composition of the film could be varied by changing the deposition conditions. Increasing the TTIP/TEOS ratio increased the Ti/Si ratio in the film, and increasing the deposition temperature decreased the Ti/Si ratio. In contrast, when the TN precursor was used, the ratio of Ti/Si was always near one, regardless of the ratio of TN/TEOS or the deposition temperature. A specific reaction between the TN and TEOS in the gas phase or on the substrate surface was proposed.

The work by Igumenov and colleagues described above [31,32] on protective coatings for titanium anodes used in seawater electrodialysis included testing a Pt/Ir composite coating. They decomposed a 50/50 (mass %) mixture of $Pt(acac)_2$ and $Ir(acac)_3$ simultaneously in the presence of oxygen at 673K. The film was composed of multiple phases; the pure metal phases, a solid solution phase, and an oxide phase (MO_2, where M is Pt or Ir). This is significant because neither the pure iridium nor platinum films contained the metal oxide; therefore the dual decomposition changed the deposition characteristics in some way.

Fourier Transform Infrared Spectroscopy Studies of CVD

Fourier transform infrared spectroscopy has been used both *ex situ* and *in situ* to study CVD systems. Ex situ generally involves examining reactor effluent [54]. Even with quenching the reaction at the reactor outlet, this method is not as useful as *in situ* FTIR because only the volatile by products can be examined, not the decomposition intermediates. *In situ* FTIR is a powerful tool for elucidating reaction pathways in the reactor [55,56]. There are several difficulties to be overcome before FTIR can be applied to a CVD system. Because of these problems, FTIR cell designs for high temperature studies, such as by Clausen and Bak [57], are unsuitable for CVD studies. The highly dilute nature of CVD systems means that very sensitive equipment with a high signal to noise ratio must be used. Alternatively, a long beam pathlength will increase the signal strength, but reduce the signal to noise ratio. The effective pathlength is the distance the beam covers through the reaction zone. It must be ensured that no deposition takes place on the infrared-transparent windows. To avoid this, the window flanges, and hence the windows themselves, can be cooled to a temperature below that which is required for decomposition. The FTIR results are also complicated, however, if unreacted precursor adsorbs on the window, because FTIR would then indicate the presence of precursor when none is flowing, or all is reacted. Therefore, if precursors that must be heated are used, the IR windows must be heated above the precursor vaporization temperature to avoid condensation on the windows. This further complicates the system, as different materials for the windows and flanges will expand at different rates when heated. This expansion can result in cracking the window, which is another reason why the window flanges are usually cooled. Finally, the evolved by-products of decomposition can adsorb

on the window. One way to essentially avoid all these problems is through the use of a complicated purging scheme to keep all species away from the windows, as done by Tachibana et al. [55]. This is space-intensive, however, and can reduce the effective IR beam pathlength.

Van der Vis et al. [58] have examined the gas phase infrared spectra of TEOS in detail. Their assignments are presented table 2.

Chu et al [54] studied decomposition of TEOS over time in a closed system. The main decomposition products were found to be ethane, ethanal, and carbon monoxide.

Van der Vis et al. [59] also examined the thermal decomposition of TEOS in a closed system. A low-pressure inert atmosphere at 800K as well as inert (800K) and oxygen (545K) atmospheric pressure atmospheres were studied. In all cases, the cell was loaded with TEOS and argon or oxygen, then closed and the decomposition proceeded with time. While this is somewhat different from a flow system, insight can be gained from their results. The decomposition products in the inert atmosphere were ethane, ethanol, methane, carbon monoxide, ethanal, and water. In an oxygen atmosphere, water, carbon dioxide, methanal, ethanal, carbon monoxide were formed.

Kawahara et al. [60] and Arno et al. [61] both studied ozone/TEOS atmospheric pressure CVD using FTIR. Kawahara used *in situ* FTIR to study a closed system (i. e. filled the cell with reactants and then measured the change over time) at lower temperatures, 330-400K. The closed system was used because they found decomposition was insignificant when the reactants were introduced in a flow system. They found the main by-products to be ethanal, methanal, carbon dioxide and water. No ethane, ethylene, or ethanol was found, in contrast to the LPCVD studies of TEOS alone

described above. In contrast, Arno et al. examined the reactor effluent downstream of the reactor, where the tubing walls were cooled to below 123K to quench the reaction. They found the main by-products to be acetic and formic acids, carbon monoxide, carbon dioxide, and water.

Whidden et al. [62] used *in situ* FTIR to study an ozone/TEOS flow system. They found the main reaction products to be acetic and formic acids, carbon monoxide, carbon dioxide and water. They also were unable to assign peaks at 1080-1200 cm^{-1} and 1745 cm^{-1}, although they suggested that the peaks around 1100 cm^{-1} may be due to Si-O-Si species in the gas phase.

The FTIR spectra of $Pt(acac)_2$ has not been specifically assigned. The assignments for the closely related $Pd(acac)_2$ have been completed [63] and are presented in Table 3. No FTIR studies on the decomposition of $Pt(acac)_2$ have been found.

Table 2. Infrared Spectra Assignments for Gas Phase TEOS [58]	
Assignment	Wavenumber (cm^{-1})
CH_3 asymmetric stretch (A′ in C_s)	2985 (vs)
CH_3 asymmetric stretch (A″ in C_s)	2985 (vs)
CH_2 asymmetric stretch (A″ in C_s)	2981 (vs)
CH_3 symmetric stretch (A′ in C_s)	2983 (s)
CH_2 symmetric stretch (A′ in C_s)	2897 (s)
CH_2 deformation (A′ in C_s)	1489 (vw)
CH_3 asymmetric deformation (A′ in C_s)	1462 (sh)
CH_3 asymmetric deformation (A″ in C_s)	1447 (w)
CH_2 wag (A′ in C_s)	1394 (m)
CH_3 symmetric deformation (A′ in C_s)	1374 (w)
CH_2 twist (A″ in C_s)	1304 (w)
CH_3 rock (A″ in C_s)	1176 (s)
CO asymmetric stretch (E in S_4)	1115 (vs)
CO asymmetric stretch (B in S_4)	1089 (vs)
CH_3 rock (A′ in C_s)	965 (s)
CH_2 rock (A″ in C_s)	805 (s)
SiO_4 asymmetric stretch (B + E in S_4)	794 (s)
CCO deformation (A′ in C_s)	478 (m)
SiO_4 deformation (A + B in S_4)	311 (vw)
CH_3 torsion (A″ in C_s)	250 (sh)

Table 3. Infrared Spectra Assignments for $Pd(acac)_2$ [63]	
Assignment	Wavenumber (cm^{-1})
ν(CH)	3070
$\nu(CH_3)$	2990
$\nu(CH_3)$	2965
$\nu(CH_3)$	2920
ν(CC) of ring + ν(CO) of ring	1569
combination	1549
ν(CC) of ring + ν(CO) of ring	1524
δ(CH) + ν(CC) of ring	1425
$\delta_d(CH_3)$	1394
$\delta_s(CH_3)$	1358
$\nu(C\text{-}CH_3)$ + ν(CC) of ring	1272
δ(CH) + $\nu(C\text{-}CH_3)$	1199
$\rho_r(CH_3)$	1022
ν(CC) of ring + ν(CO) of ring	937
π(CH)	786
π(CH)	779
$\nu(C\text{-}CH_3)$ + ring deformation + ν(Pd-O)	700
$\pi(C(CH_3)(C)(O))$	678
ring deformation + ν(Pd-O)	661
ν(Pd-O) + $\nu(C\text{-}CH_3)$	463
ring deformation	441
ν(M-Pd)	294

EXPERIMENTAL

Design of Reactor

A new low pressure chemical vapor deposition reactor was constructed. See Figure 4. Grade 5.0 argon was used as the carrier gas. Grade 5.0 oxygen was used as a co-reactant in some cases. MKS and Unit mass flow controllers were used to control gas flow rates. Bubbler-style precursor vaporizers were used for precursor delivery. The vaporization temperature of the platinum acetylacetonate, $Pt(acac)_2$, was originally controlled with heat tape. However, it was determined that this provided insufficient temperature and precursor delivery control. Hence, a custom made heater was fabricated (see Figure 5). This consisted of an aluminum cylinder with three 1/4" Watlow cartridge heaters and a thermocouple, and was controlled by an Omega temperature controller. The $Pt(acac)_2$ delivery lines were heated to approximately 15-20 K above the $Pt(acac)_2$ vaporization temperature with heat tape to avoid condensation. The heat tape temperature was controlled by a variable transformer. Sub-miniature thermocouples from Omega were attached along the delivery line with glass tape to check the temperature. Swagelok and Cajon Ultra-Torr fittings were used. An ice bath was used to cool the tetraethylorthosilicate (TEOS) to 273 K. The pressure in the TEOS bubbler was controlled with a manual needle valve and the pressure was read with a 0-1000 Torr MKS Baratron pressure transducer.

The reactor consisted of a 50 mm OD fused quartz tube capped with custom made compression-type vacuum fittings (similar to Cajon Ultra-Torr fittings). The

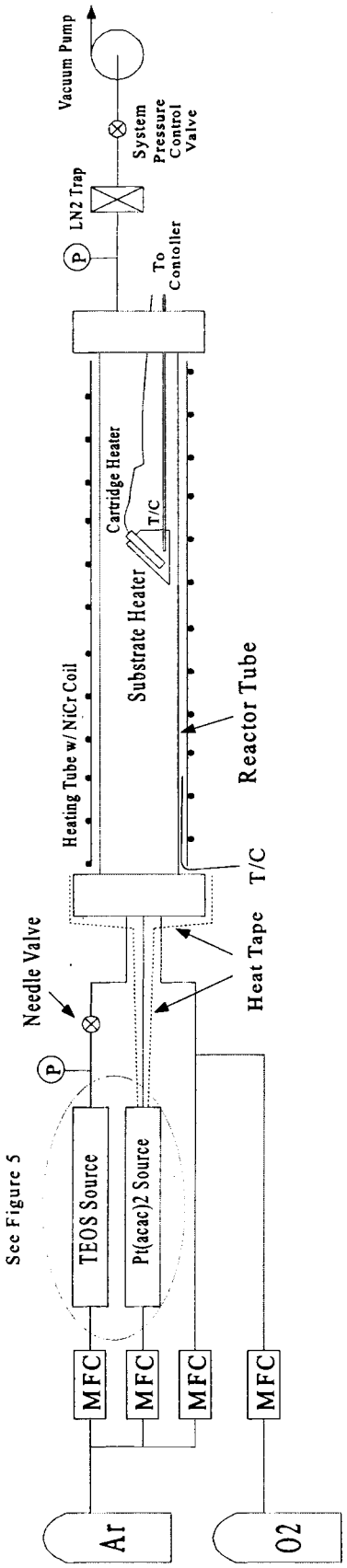

Figure 4. Schematic of Cold Wall Chemical Vapor Deposition Reactor

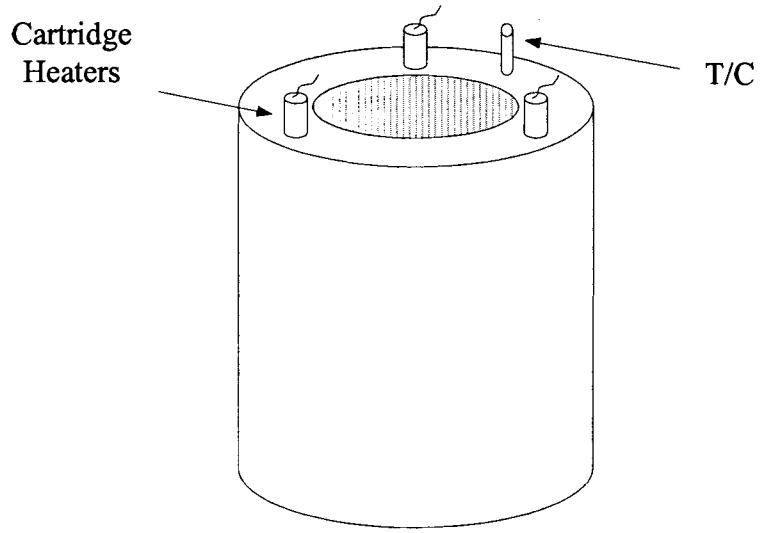

Figure 5. Heater for $Pt(acac)_2$ Bubbler

front end cap has three 1/4" NPT inlets. The precursor and co-reactant gas delivery lines were attached with Swagelok vacuum fittings.

An external heating coil for the reactor tube was constructed to avoid condensation of precursor prior to the substrate heater. This consisted of NiCr wire wrapped around a Pyrex tube of 53 mm ID. The heating coil temperature was read by placing a thermocouple between the two tubes and was controlled by a variable transformer. The heating coil temperature was hot enough to avoid condensation of the $Pt(acac)_2$ precursor, but below the temperature that would result in decomposing the precursor prior to the substrate holder. Hence, the system is known as a cold wall reactor. The substrate holder/heater was custom fabricated out of copper and has a 5 mm wide, 1 mm deep slot on the front to hold the substrate. No other means of securing the substrate was used. A 3/8" diameter cartridge heater from Watlow was used to heat the substrate holder to the required deposition temperature. The internal substrate holder

temperature was read with a 1/8" thermocouple embedded in the copper and secured with a Swagelok fitting. The temperature was controlled with an Omega controller.

The temperature at the substrate surface was found to be a function of both the heating coil temperature and the substrate holder temperature. A calibration was performed by inserting a long thermocouple through one of the front end cap ports and placing the tip directly on the substrate. While the resulting data is three dimensional (two independent variables and one dependent variable) it was found empirically that the data could be reduced to two-dimensional by defining the independent variable as the midpoint of the heating coil and substrate holder temperatures. The resulting calibration is shown in Figure 6.

The back end cap has three outlets, a 3/8", a 1/4" and a 1/8" NPT. These are for the gas exhaust, vacuum electrical feedthrough for the cartridge heater, and thermocouple, respectively. The hermetically-sealed vacuum electrical feedthrough is a

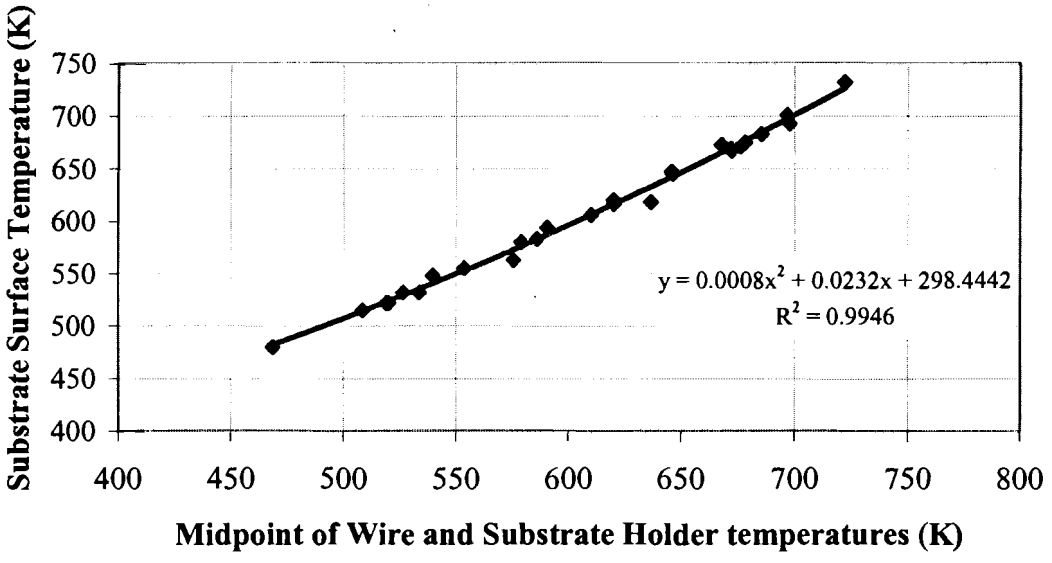

Figure 6. Calibration of Substrate Surface Temperature

stock Omega part. The reactor pressure was read by a 0-10 Torr MKS Baratron pressure transducer and controlled by an MKS control valve. The fittings for the gas exhaust pumping system were KF clamp type fittings and the tubing was 3/8" flexible tubing, both from MDC. An in-line liquid nitrogen trap was used to prevent unreacted precursor and reaction by-products from entering the vacuum pump, spoiling the pump oil and being exhausted to the laboratory atmosphere. A Leybold mechanical vacuum pump was used to pump down the system and hold it at the required pressure.

Deposition and Characterization of Platinum Films

Pure films of platinum were deposited first and the results compared to previous work to test the new reactor system. At this time, the original method of heating the platinum precursor, heat tape wrapped around the bubbler, was found to be deficient. There were hot spots where the temperature was high enough to cause the precursor to decompose on the inside of the delivery lines. At the same time, cold spots were also discovered where the precursor was condensing out of the gas phase. These problems resulted in very poor repeatability. Careful re-wrapping of the heat tape mitigated some of these problems, but it was decided that this level of control was insufficient. Therefore, the new bubbler heater, shown in Figure 5, was fabricated. This eliminated the majority of the precursor delivery problems described above. Also, the new heater made checking the level of precursor significantly easier. Previously, the heat tape had to be removed to see the $Pt(acac)_2$ powder. Doing this compromised repeatability due to the near-impossibility of replacing the heat tape in exactly the same manner. The new bubbler heater allowed the precursor level to be easily checked without repeatability concerns.

Another important concern arose while carrying out pure platinum depositions. The reactor tube did not provide a favorable deposition surface when clean, which resulted in an increased precursor yield. This was partly due to the reactor wall being at a lower temperature than the substrate, but also due to the very smooth surface of the drawn quartz tube, which did not provide favorable sites for nucleation. However, over the course of a deposition, some platinum and carbon would deposit on the reactor wall. If the tube was not cleaned prior to the next deposition, these wall deposits provided favorable nucleation sites, and deposition would rapidly occur on the reactor wall. This reduced the amount of precursor available to deposit on the substrate, and so by the third or fourth deposition without cleaning the growth rate was greatly reduced. Therefore, it was determined that it was important to clean the reactor tube after each deposition.

The cleaning regimen was to first remove as much of the deposits as possible by physical means, i. e. a standard laboratory glassware cleaning brush, then remove the remaining deposits chemically by soaking the tube overnight in aqua regia (four parts hydrochloric acid to one part nitric acid.) At times, even this did not remove all deposits. The last bits were removed by wrapping the cleaning brush in emery paper and further scrapping down the reactor walls, then soaking again in aqua regia.

Platinum films were deposited from $Pt(acac)_2$ supplied by AlfaAesar and used without further purification. Deposition temperatures were 623-693K. Depositions were carried out in a 50% oxygen atmosphere. The flow rate of the argon carrier gas through the $Pt(acac)_2$ bubbler was 25 standard cubic centimeters per minute (sccm) and the oxygen flow rate was 25 sccm. The total pressure was 1.0 Torr, which was near the lowest pressure the vacuum pump could maintain at these flows. In all cases, the

pressure of the system was reduced to below 50 mTorr before beginning each experiment. The $Pt(acac)_2$ sublimation temperature was either 393K or 403K. The precursor delivery tubing was held at 10-20K higher than the sublimation temperature to avoid condensation within the tubing. The NiCr wire temperature was always controlled to 503K ±5K, and the substrate holder temperature was adjusted to maintain the desired deposition temperature (determined by calibration, see Figure 6). The substrates consisted of single crystal r-cut sapphire cleaned in boiling acetone followed by an oxygen electron cyclotron resonance (ECR) plasma. The liquid nitrogen trap was filled before beginning precursor flow.

The platinum films were characterized by x-ray diffraction with a Scintag Diffractometer in the Geology department at the University of Maine using Cu $\kappa\alpha_1$ (λ=1.5406 A) radiation. In most cases, two-theta (2θ) scans were carried out from 5-90°.

Film thicknesses were determined by surface profilometry. First, stripes of resist (Sibley 1813) were placed on the films and hardened at 110°C. Then, the films were placed in hot (50°C) aqua regia to etch the platinum. The resist was then removed with acetone. The films were rinsed in de-ionized water and blown dry with nitrogen. This left strips of un-etched platinum and strips of blank substrate. The film thickness was determined by scanning the profilometer stylus from the film region down to the blank substrate surface. The profilometer was a Tencor Alpha-step 200. Growth rate was then determined by dividing by the growth time. Film thickness uniformity was also determined by measuring each film at six spots. It was determined that repeatability was attained when the growth rate at set conditions varied by less than 10%.

Deposition and Characterization of Composite Films

Once repeatable growth of platinum films was attained, the TEOS line was added to the delivery system. At the same time, a makeup argon line was also added. The makeup line allowed for changing the oxygen flow rate but still maintaining the same total gas flow rate, and therefore, the relative precursor concentrations.

$Pt(acac)_2$ was sublimed at 403K and carried into the reactor by 25 sccm argon. TEOS was vaporized at 273K and carried into the reactor by 5 sccm argon. The pressure in the TEOS bubbler was maintained at 30 Torr. The oxygen flow rate was between 0-70 sccm and the makeup argon was between 0-70 sccm, so that the total gas flow rate into the reactor was always 100 sccm, plus a negligible amount of precursor. Depositions were carried out at 1.6 Torr in the temperature range 573-713K. The same substrates, r-cut sapphire, were used for depositing composite films.

No measurement of the concentration of precursors was made, so Equation 1 on page 5 is the only guide for the relative amounts of each precursor that were flowing into the reactor. From Equation 2, the vapor pressure of TEOS at 273K is 0.28 Torr. From Equation 1, the flow of TEOS into the reactor is 0.047 sccm. Similarly, the vapor pressure of $Pt(acac)_2$ at 403K is 0.0084 Torr. Assuming that the pressure in the $Pt(acac)_2$ bubbler is the same as the reactor pressure and that the carrier gas is saturated, the flow of $Pt(acac)_2$ would be 0.13 sccm. Therefore, the ratio of TEOS to $Pt(acac)_2$ would be 0.36. In reality, both of these assumptions are suspect. It is likely that the pressure in the bubbler is slightly higher than the reactor pressure, which would slightly decrease the expected precursor flow rate, and that the carrier gas stream is not saturated with $Pt(acac)_2$, which could significantly lower the precursor flow rate. Therefore, it is

expected that there is an excess of TEOS flowing into the reactor, though no measurement was made to confirm this. The ratio was variable in any case, due to the well known problems associated with solid precursors described above.

The film compositions were determined me in a SPECS X-Ray Photoelectron Spectroscopy (XPS) system at the Laboratory for Surface Science and Technology at the University of Maine after being cleaned in a low energy Ar ECR plasma to remove the majority of absorbed species with removing any of the film. The data was analyzed using SPECS software. Finally, film growth rates were determined by surface profilometry in the same manner as for the platinum films. In most cases, this procedure was sufficient to etch the film, but a few films required an etch in HF following the etch in aqua regia. The resist was then removed in the same manner as described above.

In Situ FTIR Study

A schematic of the equipment setup for this study is shown in Figure 7. Several modifications to the reactor system were required to carry out the *in situ* FTIR study. The infrared beam had to pass unobstructed through the reactor cell. Therefore, infrared-transparent windows had to be held in place at the ends of the reactor. The window material used for these experiments was NaCl, because of its low cost and sufficient transmission range. The windows had to be heated to avoid condensing unreacted precursor on them. This and the required vacuum seal were the two critical design considerations. These problems were solved with the end cap design shown in Figure 8. The end cap material was stainless steel. It consists of a compression-type vacuum seal to the reactor tube, similar to the end caps used in the deposition experiments above. The

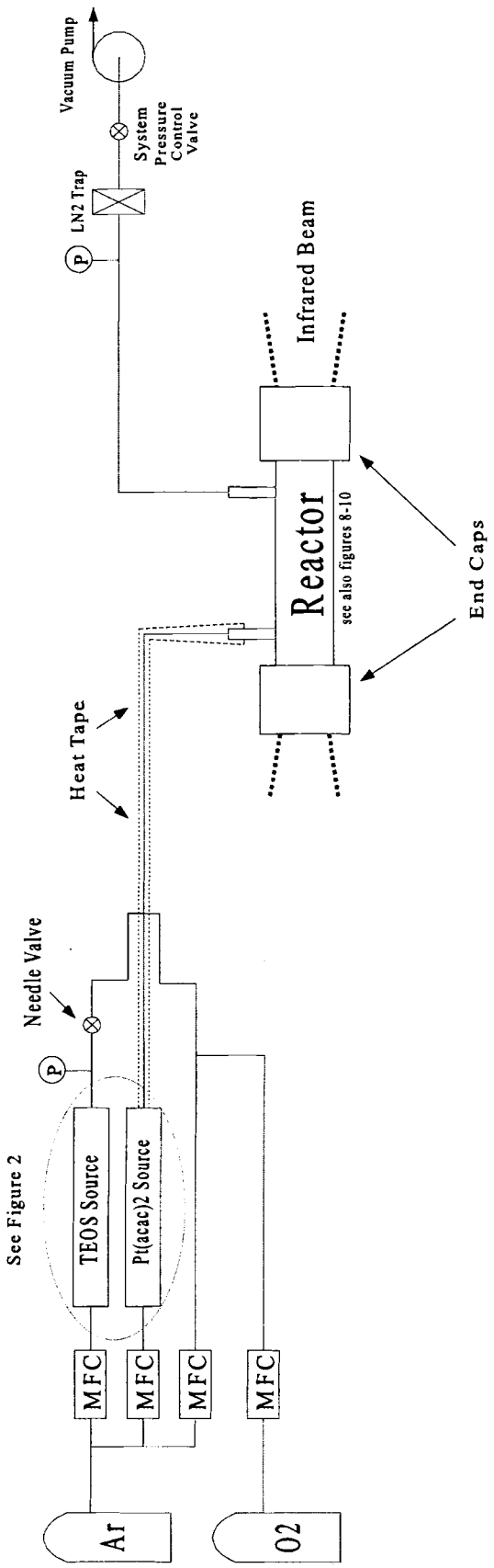

Figure 7.
Schematic of Hot Wall CVD Reactor for FTIR Study

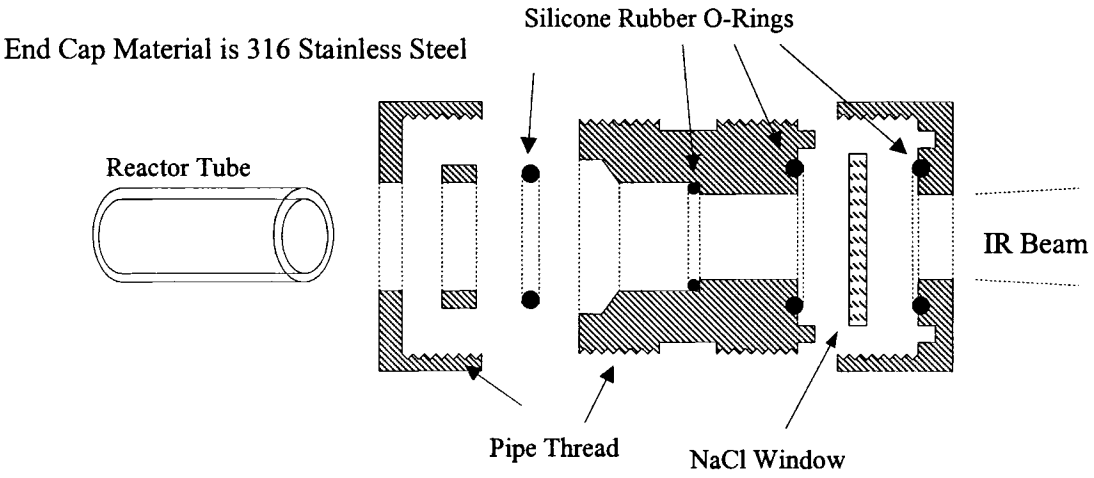

Figure 8. Cross Section of End Cap

infrared transparent window was held in place by two face-seal o-rings, the inner one of which provided the vacuum seal and the outer one which provided cushioning. The end caps and the windows had to have the capability to be heated as high as 473K. The different thermal expansion rates of the window material and end cap material could result in cracking the window. The face seal o-ring design allowed sufficient cushioning so that the windows could be heated without cracking.

A diagram of the reactor tube is shown in Figure 9. The reactor and gas ports consisted of fused silica tubing. Since the infrared beam had to pass straight through the reactor, the end caps were no longer available for the introduction and exhaust of reaction gases from the reactor. Therefore, gas inlets and outlets were attached directly to the reactor tube. This necessitates pre-mixing all components entering the reactor prior to the gas inlet port. In this way, the new reactor was different than the previous design, in which the reactants did not meet until in the reactor. NiCr wire was again used to provide the heating. Insulation, consisting of alumina-silicate ceramic fibers with an organic

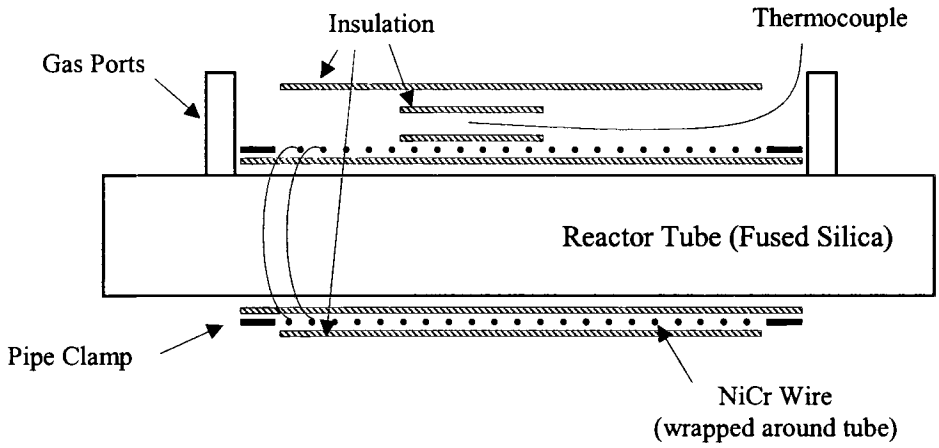

Figure 9. Cross Section of Reactor

binder, was wrapped around the central section of the reactor tube and held in place by pipe clamps. The NiCr wire was then closely wound around the tube and hooked on the pipe clamps on both ends. A sub-miniature thermocouple from Omega was wrapped with the same insulation and placed on top of the NiCr wire to read the reactor temperature. Another layer of the alumina-silicate insulation was then applied and held in place by high temperature string. The organic binder must be burned out of the insulation in a fume hood prior to using the reactor in a lab environment. The reactor temperature was controlled by an Omega temperature controller in concert with a Variable transformer variable transformer.

The spectrometer was a Bomem MB-Series and the data capture and analysis software was Bomem GRAMS. The detector was a liquid nitrogen cooled MCT. The resolution was 4 cm^{-1}. The custom designed end caps described above resulted in a reactor length longer than could fit between the source and detector modules on the spectrometer, which had F4 optics. Therefore, F10 optics were used to increase the

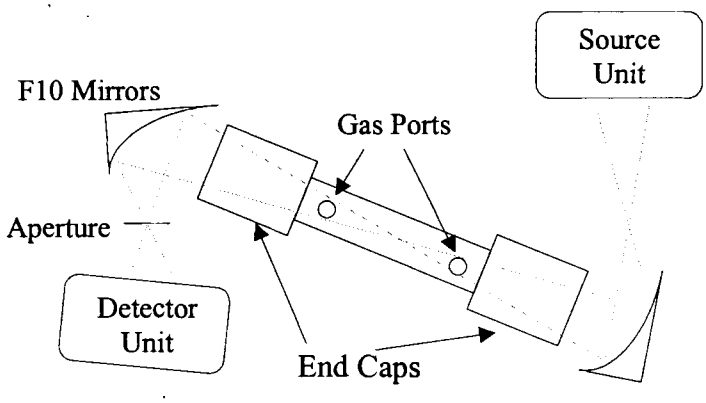

Figure 10. Top-Down View of Reactor with Spectrometer Equipment

pathlength beyond the length of the reactor. Unfortunately, this necessitated aligning the infrared beam manually, and meant that a slight movement in the optics or detector module would compromise the alignment. Therefore, a platform was constructed consisting of an anodized aluminum optical board predrilled with 1/4" NPT holes for securing the components. In addition, an aperture was placed between the second mirror and the detector to reduce the affect of scattering for the TEOS/$Pt(acac)_2$ study . A top down diagram of the reactor and spectrometer is shown in Figure 10.

In each case, the region 4000 – 600 cm^{-1} was scanned. One hundred scans were averaged to increase the signal/noise ratio in all cases. The decomposition temperature was varied between 473-873K for the pure platinum runs and over 473-773K for the composite runs. The oxygen content was either 0% or 70% for the platinum runs and always 70% for the composite study. The pressure was 1.6 Torr. In all cases, $Pt(acac)_2$ was vaporized at 403K and carried into the reactor by 25 sccm of argon. For the composite study, TEOS was vaporized at 273K and carried into the reactor by 5 sccm of argon. The pressure in the TEOS bubble was maintained at 30 Torr and the TEOS was

kept in an ice bath. The delivery lines after the $Pt(acac)_2$ bubbler were heated to 15-20K above the bubbler temperature to avoid condensation. The reactor end caps were held at 165-175K to avoid condensation of $Pt(acac)_2$ on the NaCl windows. Three readings were taken at each temperature for the $Pt(acac)_2$ decomposition study, one immediately upon starting the precursor flow, one after 10 minutes, and one after 20 minutes, when the reactor should have attained steady state. For the TEOS/$Pt(acac)_2$ study a scan was taken at the start of flow and another after 20 minutes. Each scan took approximately 3 minutes to complete. The long time to reach steady state was due to the large "dead" volumes in front of the NaCl windows. The system was purged after the run at each temperature. The purging procedure was to turn off the precursor and oxygen flows and allow argon to flow for a period of time. The argon was then shut off and the reactor pumped down to approximately 50 mTorr. Argon was then again flowed, followed by pumping the reactor down again. This cycle was done up to five times while the reactor was heated up to the next decomposition temperature. Spectra were then taken to ensure that no chemical species remained in the reactor. If there was still some reactant present, the reactor was purged further. A reference was taken at each temperature with the process gases flowing, but no precursor flowing. This was done to reduce the influence of any species that may have absorbed on the windows during the previous run.

RESULTS AND DISCUSSION

Composite Film Deposition

A set of depositions was carried out at 673K varying the oxygen content of the atmosphere between 0-70%. Growth rates varied from 1-4.4 nm/min. Films varied in reflectance, with low-carbon films being smooth and mirror-like and high-carbon films being rougher and unreflective. Color was also dependent on the carbon content of the film, where low-carbon films were nearly the same color as pure platinum films, and high-carbon films were dark grey. Color was independent of silicon content of the films. XRD analysis determined that the platinum phase of the films is crystalline and randomly oriented, and that the silica phase is amorphous, as expected (see Figure 11).

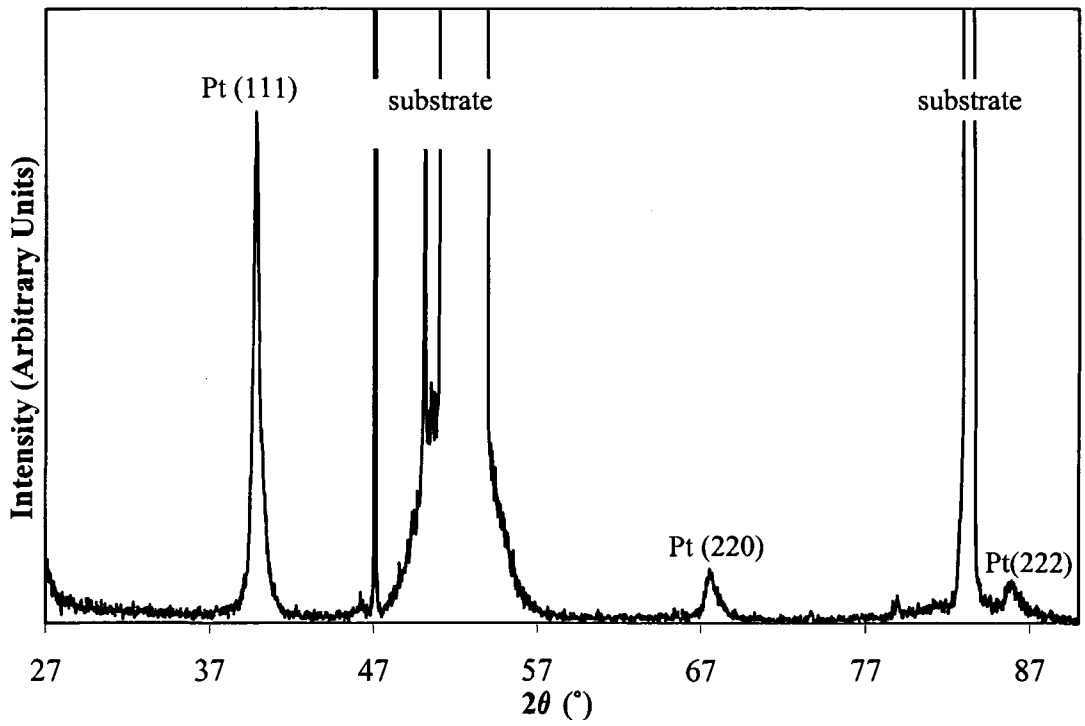

Figure 11. Representative X-Ray Diffraction Pattern of Composite Film Grown at 673K in 70% Oxygen. Expected peaks and intensities for polycrystalline platinum are present, no peaks for any silicon dioxide are present.

The results of XPS analysis of the deposited films are presented in Figure 12. The atomic percentages of the four constituents of the film, platinum, silicon, oxygen and carbon, are shown against the oxygen content of the growth atmosphere. The presence of oxygen has a marked affect on the film composition. A small amount of oxygen is required to have silicon incorporation into the film. Increasing the oxygen from 0% to 10% increases the amount of silicon from near zero to 14% of the film. The percentages of silicon and platinum approach each other as the flow of oxygen is increased; this effect

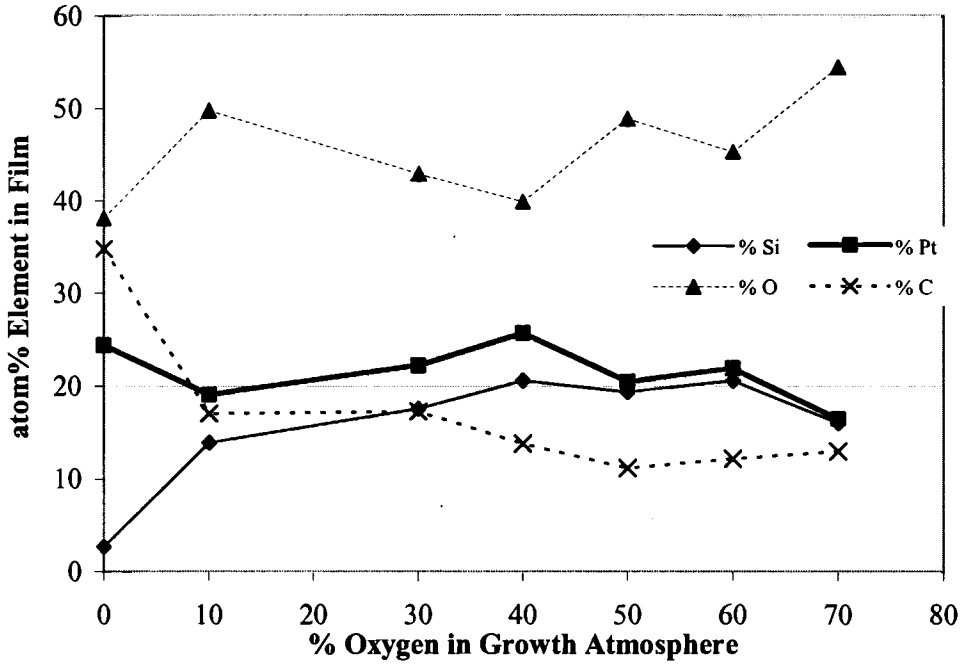

Figure 12. Affect of Growth Atmosphere on Composite Film. Atomic percentages of each component are shown as the amount of oxygen in the growth atmosphere is varied between 0-70%.

is better shown in Figure 13 as a ratio of the two percentages. As found by previous researchers[23,26], the deposition of platinum from $Pt(acac)_2$ results in high carbon content films. The amount of carbon drops from 35% to 18% with just 10% oxygen, and drops

slightly more with additional oxygen. This is more carbon than found by previous work when $Pt(acac)_2$ is decomposed with oxygen, 0-2% [24, 25, 26, 30, 29], although Barison et al.[64] found approximately 16% carbon in the platinum films after sputtering the film surface off when the films were grown in oxygen or other reactive atmospheres. The large amount of carbon may indicate the composite deposition process did not allow for the complete removal of precursor ligands, although the equipment was limited to relatively low temperatures. The percentage of oxygen in the films does not appear to follow any definite trend. However, oxygen is difficult to remove from the UHV system, and even after sputtering the film in a Ar ECR plasma, oxygen can again adsorb onto the film prior to examining it in the XPS. Therefore, the error in this measurement is expected to be significant.

Figure 13 shows the atomic ratio of silicon/platinum versus the oxygen content of the growth atmosphere. This ratio is near 0.1 with no oxygen flow. Adding O_2 greatly

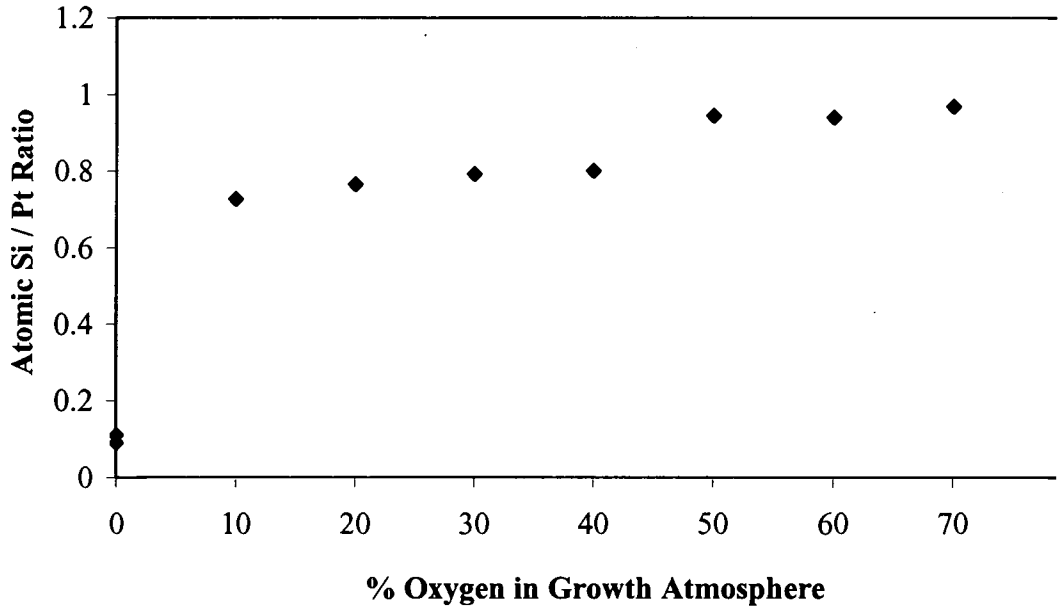

Figure 13. Affect of Oxygen on the Si/Pt Ratio in Composite Films

increases the ratio, with an increase from 0% to 10% O_2 resulting in a Si/Pt atomic ratio of about 0.75, and further increasing the oxygen composition to 70% results in a Si/Pt ratio approaching 1.0. The growth rate was found to be independent of O_2 content above 10%. No growth rate could be measured at 0% O_2 because the films delaminated from the substrate when the film thickness measurement procedure outlined above was followed. This indicates that the film grown without oxygen is of low quality.

There was no deposition from TEOS alone at these conditions, neither on the r-cut sapphire substrates nor on a sapphire substrate pre-coated with platinum, even if the O_2 was increased to 95%. If the flow of $Pt(acac)_2$ was stopped, no further deposition occurred, consistent with previous studies.

A second set of experiments was carried out in which the deposition temperature was varied from 573K to 713K. The results are presented in Figure 14. The O_2 flow was

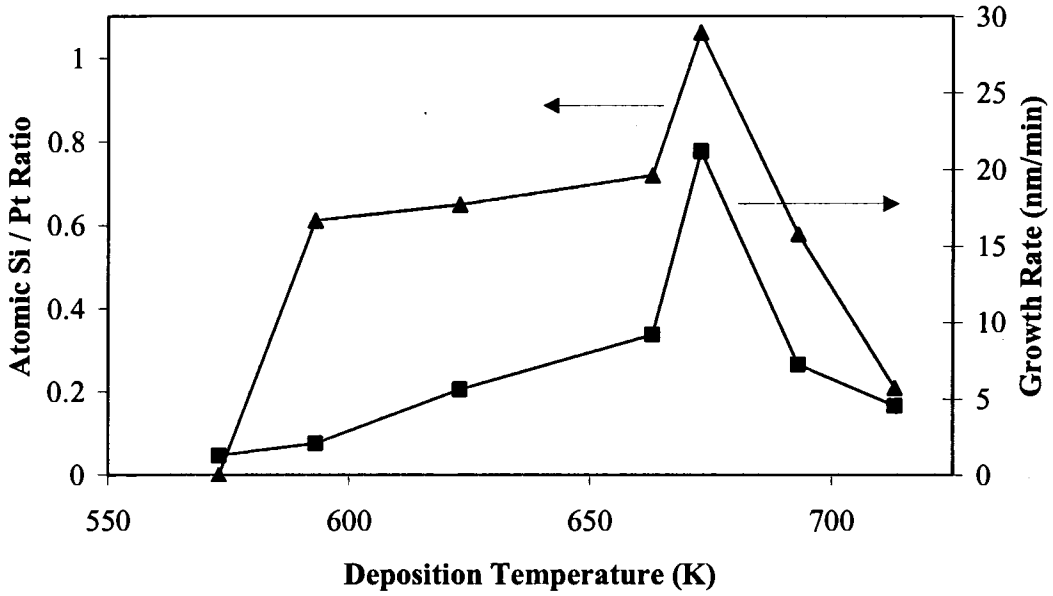

Figure 14. Film Composition and Growth Rate with Deposition Temperature. Both the Si/Pt ratio and the growth rate peak at 673K.

set at 70% of the total, with other growth conditions the same as described above. There was incorporation of silicon dioxide into the film at temperatures as low as at 593K. The atomic ratio of silicon to platinum in the film increased from 0.6 at 593K to a maximum of near 1.0 at 673K, and then decreased to 0.2 at 713K, which was the maximum deposition temperature that could be maintained in the reactor. The same figure also shows the growth rate, which increased from 1.3 nm/min at 573K up to 21.2 nm/min at 673K, then decreased to 4.5 nm/min at 713K. The decrease in growth rate above 673K can be partially explained by the reduced rate of silica incorporation, which is explained further later. It has been reported that the growth of platinum from $Pt(acac)_2$ changes from kinetically-controlled below 668K to diffusion-controlled above 668K[28]. This coincides with the decrease in silicon content of the films above 673K.

It is well known that the delivery rate of vapor from solid precursors is difficult to control[2]. At the same deposition temperature and oxygen flow, growth rates varied considerably, *but the composition did not.* For instance, it was found that films grown at 673K and 70% O_2 were limited to a Si/Pt ratio of 1.0, independent of the film growth rate. This shows that at these conditions, the incorporation of SiO_2 is self-limiting, irregardless of the ratio of precursors fed to the reactor.

Previous work by Hochberg et al.[22] and Desu[12], described in detail above, provides insight into the possible reaction mechanism leading to the low temperature decomposition of TEOS. Their work leads to the theory that in the presence of oxygen, the decomposition of $Pt(acac)_2$ produces free radicals, which then react with the TEOS, leading to silica deposition. This could explain the low temperature decomposition of TEOS. It can not, however, account for the fact that the ratio of silicon to platinum in the

film is self limiting at one to one over a range of conditions. Pyrolysis would likely produce more than one free radical for each $Pt(acac)_2$ molecule that is decomposed. If the TEOS was reacting with the small organic free radicals, the ratio of silicon to platinum in the films would likely be greater than one to one. Also, this theory can not explain why the amount of silicon in the films is reduced at temperatures greater than 673K. More free radicals would be produced at higher temperatures, in which case, if this theory were correct, the ratio of silicon to platinum should again be greater than one to one.

A more likely explanation is that the $Pt(acac)_2$ partially decomposes in the gas phase, then forms a complex with the TEOS. This intermediate complex then absorbs to the surface and decomposes to the Pt/SiO_2 film. The platinum intermediate that reacts with TEOS is only formed in the presence of oxygen, and is short lived at temperatures above 673K. This mechanism would account for the self-limiting composition of the films and the reduction in silicon content observed above 673K. Gladfelter et al. [49] proposed a similar mechanism when they found that CVD of $Ti_xSi_{1-x}O_2$ from TEOS and titanium tetranitrate (TN) also resulted in films with Ti/Si ratio of one to one.

FTIR Study

The *in situ* FTIR study was undertaken for three reasons; to attain independent evidence of the low temperature decomposition of TEOS, to examine the decomposition pathway of $Pt(acac)_2$ under a range of deposition temperatures and oxygen flows, and finally to elucidate the catalytic-like mechanism behind the low temperature decomposition of TEOS. The individual spectra of TEOS and $Pt(acac)_2$ were first taken for reference and these are shown in Figure 15. The absorbance scale is not the same for

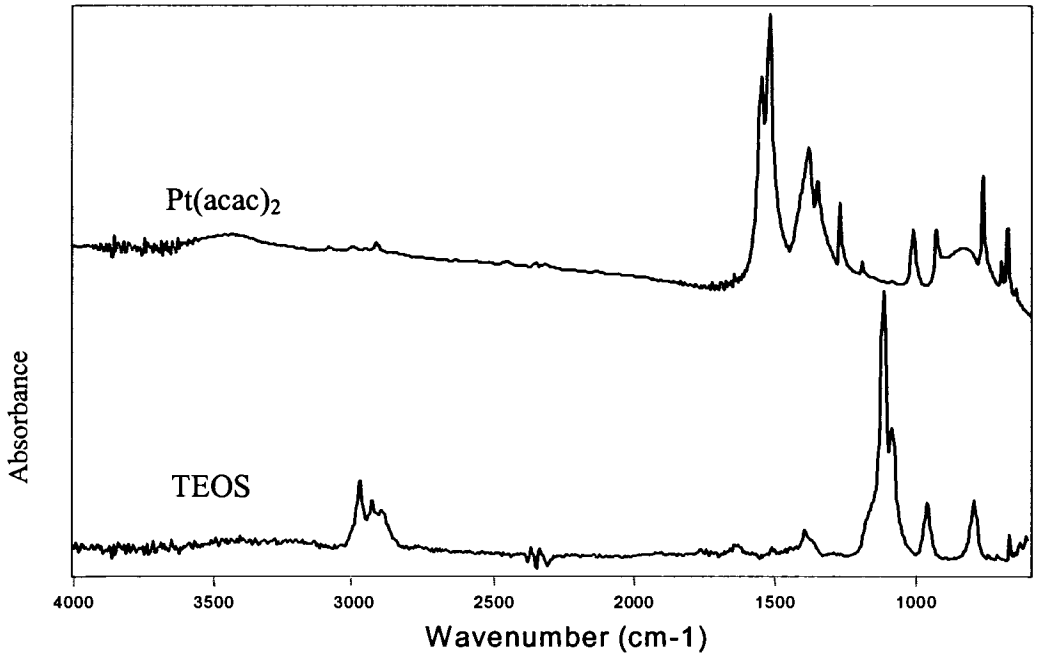

Figure 15. Precursor Spectra, Solid $Pt(acac)_2$ and Gas-Phase TEOS

the two spectra, which are offset for clarity. The TEOS spectrum was taken in the FTIR CVD reactor, which was held at 473K and 10 Torr. The TEOS was vaporized at 273K and carried into the reactor by 5 sccm Ar. The spectrum of solid $Pt(acac)_2$ was taken by mixing the powder with KBr and pressing it into a pellet. Peak assignments for TEOS are provided in Table 2 and for the related $Pd(acac)_2$ in Table 3. The two chemicals should be easy to identify when both are present because the major peaks of $Pt(acac)_2$ are in the region 1570-1525 cm^{-1} and of TEOS are in the regions 2900-3000 cm^{-1} and 1115-1089 cm^{-1}.

The *in situ* FTIR spectrum of TEOS alone in the CVD reactor is shown in Figure 16. The spectra were taken at reactor temperatures of 473-873K, in 70% oxygen flow, and at 1.6 Torr. The absorbance scale is the same for all the spectra, and this will be true for all subsequent spectra presented. Figure 16 also shows that the main peaks ascribed to TEOS are reduced in size at 673K and further reduced at 873K. This can be partially

attributed to the reduction in concentration due to the increased reactor temperature, but there was likely some interaction with species remaining in the reactor after purging and with platinum deposited on the walls by the previous experiments. The set of peaks centered at 2350 cm^{-1} are due to atmospheric carbon dioxide. The "noisy" appearance of the data at approximately 1480-1600 cm^{-1} and above 3200 cm^{-1} is due to atmospheric water vapor. An attempt was made to reduce the influence of these atmospheric species by spectral subtraction using the BomemGRAMS software. Previously taken spectra of carbon dioxide and water were used to offset the peaks in the captured data. This is not a perfect procedure, hence the noisy appearance of the data.

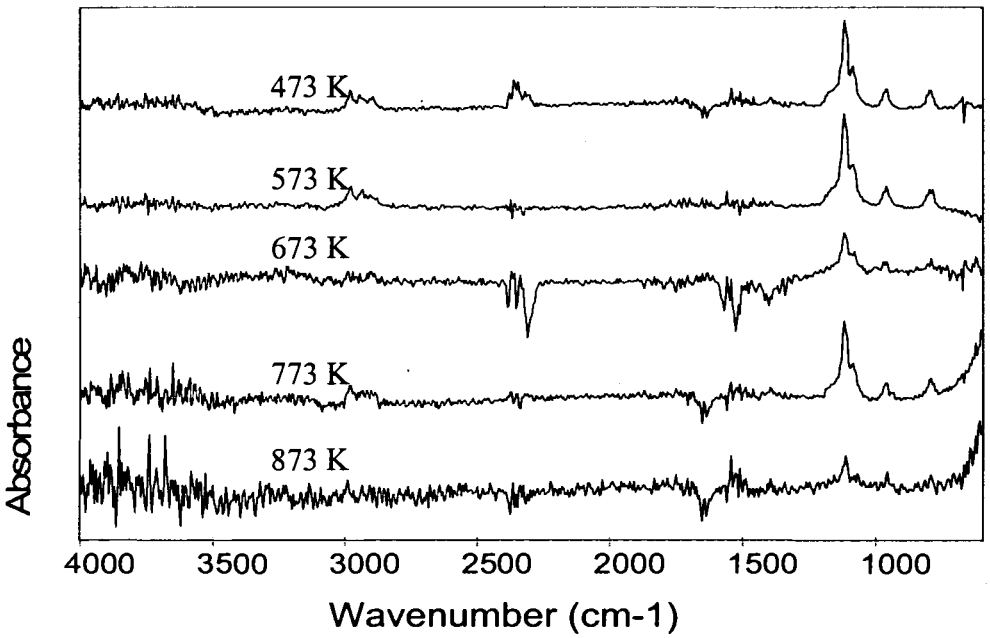

Figure 16. TEOS Spectra at Each Decomposition Temperature.
TEOS alone in the CVD reactor, water and CO_2 peaks subtracted.

Figure 17 shows results which satisfy the first goal of the FTIR study, which was independent confirmation of the low temperature decomposition of TEOS in the presence

of $Pt(acac)_2$ and O_2. Shown are two spectra taken at a reactor temperature of 773K and 70% oxygen. The top one is the spectra of TEOS alone at these conditions. The main peaks are indicated. The bottom spectra shows the result immediately after starting the flow of $Pt(acac)_2$. The TEOS peaks are nearly gone, indicating that the majority of the TEOS is reacting and being removed from the gas phase. This is striking evidence for the low temperature decomposition of TEOS.

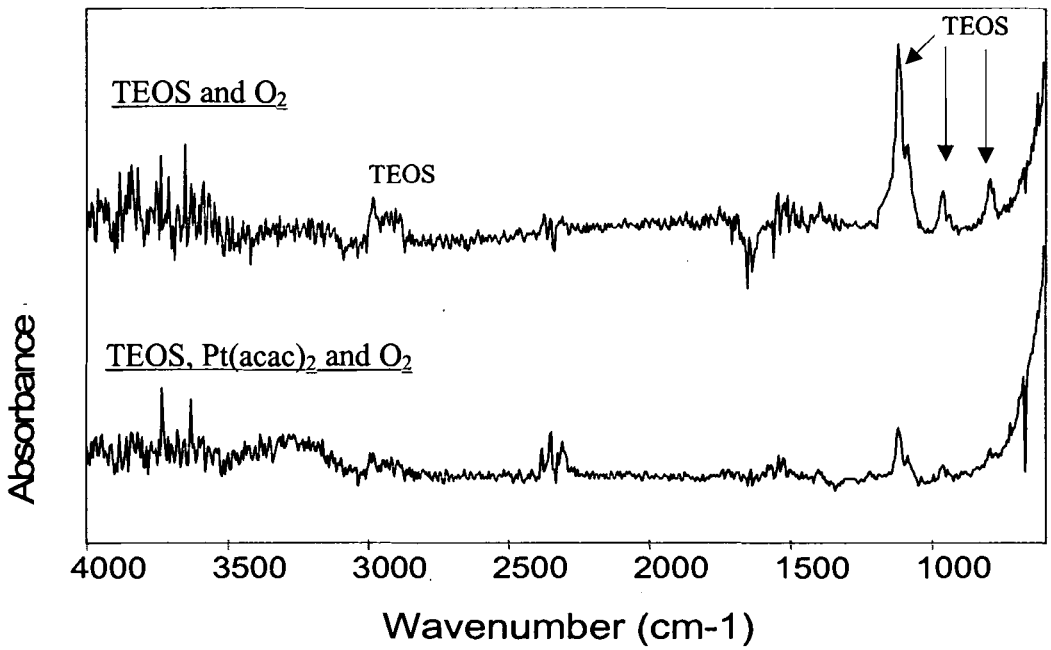

Figure 17. Decomposition of TEOS with $Pt(acac)_2$ at 773K and 70% O_2. Direct evidence of the low temperature decomposition of TEOS in the presence of $Pt(acac)_2$ and O_2.

The complete range of temperatures tested is shown in Figure 18. These spectra were all taken after 20 minutes of $Pt(acac)_2$ flow. The spectrum taken at 473K shows the presence of both $Pt(acac)_2$ and TEOS. The one at 573K shows TEOS but no $Pt(acac)_2$, showing that $Pt(acac)_2$ reacts at this temperature. The spectra taken at higher

temperatures show only very small $Pt(acac)_2$ and TEOS peaks, if any at all. It is of interest to note that the spectra taken at 773K and 873K show what may be evidence of the reduction in silica in the films grown above 673K. The very weak doublet that appears at the strongest absorption of TEOS at 1115 and 1089 cm^{-1} may indicate the

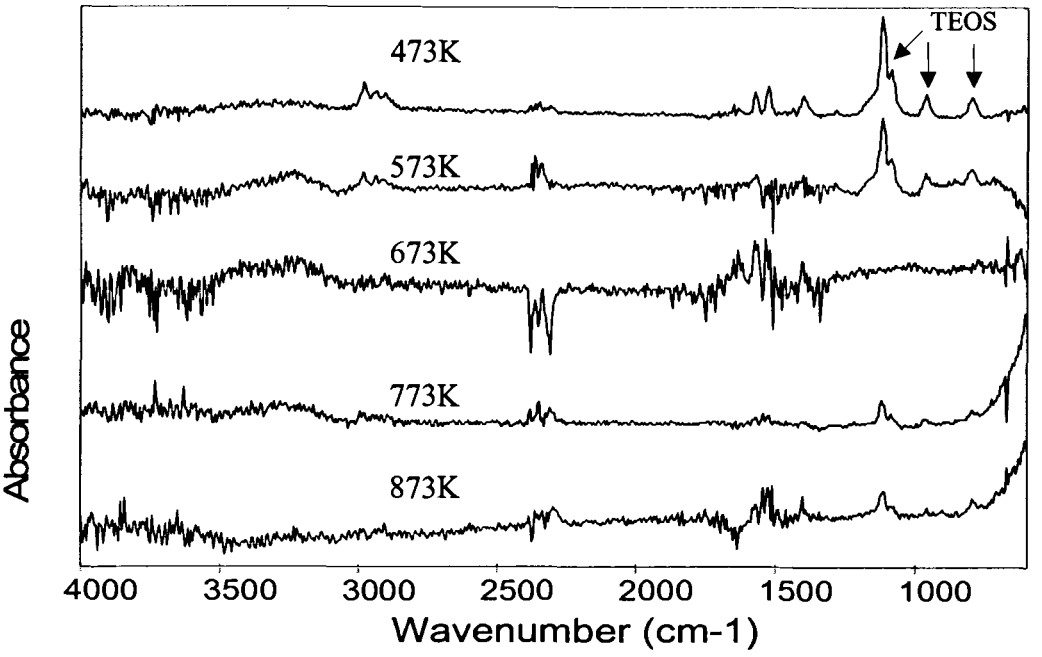

Figure 18. TEOS and $Pt(acac)_2$ after 20 min in 70% O_2 at 473-873K. TEOS is completely decomposed at 673K, but some is present at higher temperatures.

presence of unreacted TEOS. This may provide proof that at elevated temperatures less TEOS is decomposed, as was shown in Figure 14.

The next goal, determining the decomposition pathway of $Pt(acac)_2$, proved more difficult. The decomposition of $Pt(acac)_2$ in the absence of TEOS with and without oxygen was examined. It was discovered that without oxygen a large amount of "soot" is produced, which is consistent with the high carbon films produced in the absence of oxygen. This soot fogged the NaCl windows severely, and no usable data could be

obtained. Decomposition in the presence of oxygen did not produce this soot. Figure 19 shows the results of decomposition in 70% oxygen at 573K. A spectrum was taken immediately upon starting the $Pt(acac)_2$ flow, after 10 minutes and after 20 minutes, keeping in mind that 100 scans are averaged to make each of these spectra, and this takes approximately three minutes to take. The main peaks of $Pt(acac)_2$ are clearly visible at 1570 and 1525 cm^{-1} when the flow is first started. These diminish as the system approaches steady state, and are

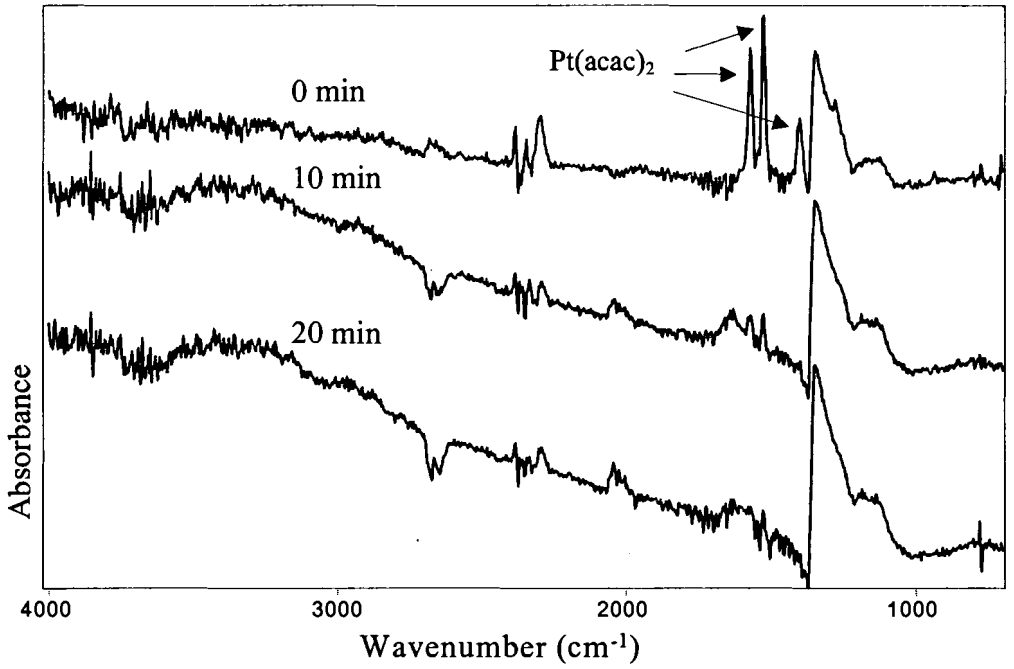

Figure 19. $Pt(acac)_2$ at 573K in 70% O_2 at 0, 10, and 20 minutes. The key peaks of $Pt(acac)_2$ indicated disappear after 20 minutes, indicating it is all reacting.

considerably smaller after 20 minutes of operation. This is partly due to the fact that a pulse of precursor moves through the system when the $Pt(acac)_2$ bubbler is first opened. The peak at 1330 cm^{-1} is due to the adsorption of silica from the inner walls of the reactor tube. No aperture was used to filter out the infrared radiation scattered off the inside

walls of the reactor. The somewhat broad peak at 1600 cm^{-1} is due to adsorbed water, either on the NaCl windows or the reactor tube walls. The peaks at 2670 and 2030 cm^{-1} are due to insufficient purging of the reactor between runs, and are not related to the true decomposition pathway of $Pt(acac)_2$. The fact that the peak at 2670 cm^{-1} "goes negative" indicates that the species causing this absorption was present when the reference spectrum was taken, and was not present when data spectrum was taken. It appears to be converted to a platinum-carbonyl species, the likely cause of the peak at 2030 cm^{-1}. The peaks centered at 2350 cm^{-1} are due to carbon dioxide. There are not any peaks significant enough to provide information on the decomposition of the precursor.

Figure 20 shows data for the decomposition of $Pt(acac)_2$ alone at reactor temperatures of 573-873K. The only obvious features observed are the artifacts at 2670, 2350, 2030, 1600, and 1330 cm^{-1} that have already been identified. The peaks at 2670 and 2030 cm^{-1} do not follow any apparent pattern; the fact that they appear randomly supports the conclusion that they are artifacts and not true decomposition products. The main $Pt(acac)_2$ peaks at 1570 and 1525 cm^{-1} are still present at 723K , but seem to be completely gone at 773K and above, indicating all the precursor has been decomposed. Further experimentation is required to determine the decomposition pathway of $Pt(acac)_2$.

An attempt can be made to satisfy the third goal of elucidating the catalytic-like mechanism based on the limited information gained from composite thin film deposition, the infrared study, and previous work done by others [35,37]. A possible reaction scheme in the presence of oxygen is shown in Figure 21. In the first step $Pt(acac)_2$ partially decomposes to a reactive intermediate, proposed here as Pt(acac). This is supported by the work of Stryckmans et al [37] with $Mg(acac)_2$ as well as work by Hierso et al [35] with the

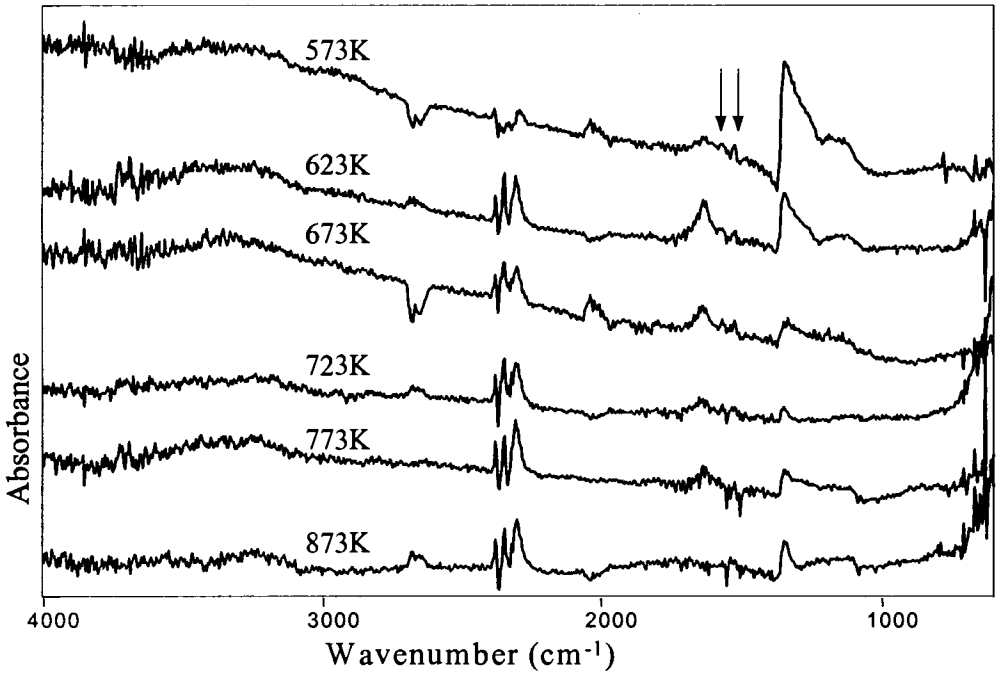

Figure 20. Decomposition of $Pt(acac)_2$ in 70% O_2 at 573-873K. All precursor is reacted at a temperature of 773K and above, as indicated by the disappearance of the indicated peaks.

related $Pt(hfa)_2$ showing that the entire acetylacetonate ligand tends to dissociate from the metal intact. TEOS reacts with this platinum species to form a silicon-platinum-organic species that subsequently adsorbs onto the substrate surface. The structure of this intermediate is entirely speculative. This reaction is supported by the finding that the ratio of silicon to platinum in the composite films is self limiting at one to one over a range of conditions. This complex then decomposes to leave behind a platinum/silica composite film. The large amount of carbon present in the films indicates the ligands are not being completely removed.

The low temperature decomposition of TEOS may also be due to TEOS reacting with acetylacetonate free radical. This theory is supported by the work of Desu [12] which predicts that TEOS would decompose at lower temperatures if reacted with radicals more

stable than the ethyl radical ($.C_2H_5$). The problem with this theory is that more than one radical is likely produced by the decomposition of $Pt(acac)_2$, and so there should be more silicon than platinum in the films if this were the case.

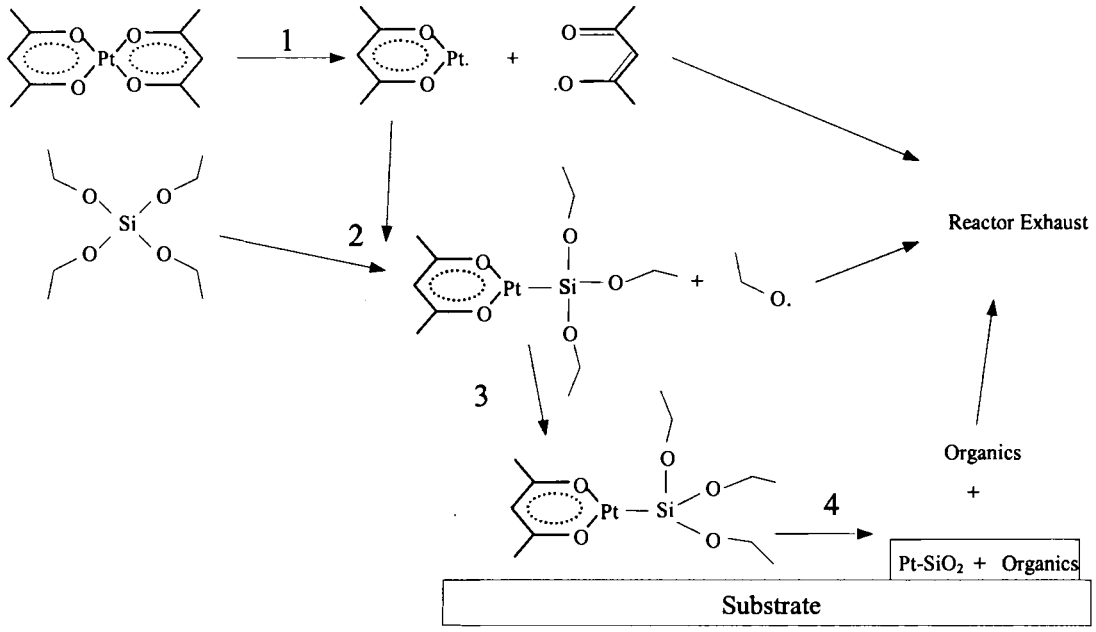

Figure 21. Proposed Scheme for Reactions Leading to the Low Temperature Deposition and Self-Limiting Composition of Platinum/Silica Films from TEOS and $Pt(acac)_2$

CONCLUSION

The low temperature deposition of silica from TEOS to form composite films of platinum and silica has been demonstrated. The simultaneous chemical vapor deposition of TEOS and $Pt(acac)_2$ in the presence of oxygen has been shown to reduce the decomposition temperature of TEOS to as low as 573K. In addition, the composition of the films is self-limiting at a one to one ratio of silicon to platinum over a wide range of conditions. This effect has been explored for varying oxygen flow rates and deposition temperatures. A new low pressure cold wall chemical vapor deposition reactor was constructed to carry out this study.

An *in situ* Fourier transform infrared spectroscopy study was undertaken. New equipment was fabricated to meet the demands of this study. Additional proof of the low temperature decomposition of TEOS was obtained by infrared spectroscopy. Further experimentation is required to determine the decomposition pathway of $Pt(acac)_2$ and how this results in the low temperature decomposition of TEOS, as well as the self-limiting composition of the films. A reaction scheme has been proposed based on the results of this work and previous work of others that could account for the observed catalytic-like affect and one to one ratio of silicon to platinum in the films.

This work has implications beyond the production of platinum/silica composite thin films, or even other metal/silica composites. It demonstrates how gas-phase reactivity may be used to reduce the deposition temperature of a certain precursor to allow its use on substrates that may only be heated to a limited temperature. Reducing the deposition temperature has other advantages as well, including less stress in the films upon cooling to service temperatures. Perhaps more importantly, this work shows how

the composition of films grown by CVD could be controlled by gas-phase reactivity and interactions between precursors. In addition to the elaborate control schemes now employed to make composite thin films by CVD, such as in the production of thin film high temperature superconductors, perhaps precursors could be fabricated that would allow for stoichiometric composition with less concern for delivery control. In all, the gas-phase reactivity of CVD precursors is an area that has not been widely explored yet could yield large gains in future work.

FUTURE WORK

Future work in this area could follow several different paths. First, the use of other metal acetylacetonate precursors, such as $Cr(acac)_3$, $Cu(acac)_3$, or $Ir(acac)_2$, could be explored. Platinum(II) hexaflouroacetylacetonate, $Pt(hfa)_2$, should also be examined to see if it provides the same affect on TEOS. If my theory is correct, these should all provide the same catalytic-like effect and self-limiting film composition as $Pt(acac)_2$.

The affect of additives is another possible area of exploration. The use of pure acetylacetonate with TEOS should be examined to determine if the catalytic effect is due solely to the precursor ligand. My theory would be proven incorrect if the same low temperature decomposition of TEOS is achieved with acetylacetonate as with $Pt(acac)_2$. Also, free radical inhibitor molecules, such as triphenylmethane, could be added. This may show if the TEOS is reacting with organic free radicals instead of the platinum compound. However, any reduction in silica incorporation could also be explained by the inhibitor molecule binding with the platinum compound in place of TEOS, so this may not be of great use.

Finally, the infrared study could be refined. The key improvement to the equipment would be the incorporation of argon purging in front of the NaCl windows. With this addition, the adsorption of reactants and by products onto the windows would no longer be a concern. Therefore, the decomposition of $Pt(acac)_2$ without oxygen could be explored to determine why the catalytic affect on TEOS is not observed in this case. Other improvements could also be made to the FTIR system. Since the mirrors, reactor, and detector were all aligned manually, the alignment was not as good as it could have been. Having the components aligned better would result in a higher signal/noise ratio,

so smaller peaks could be observed. The reactor should be also be more tightly secured against slight vibrations that arise from opening and closing the manual valves of the precursor delivery system. An improved purging scheme should be implemented to better clear the reactor of all gases between experiments at different conditions. This would aid in determining the by products of $Pt(acac)_2$ and TEOS decomposition. A wider wavenumber range would be useful, particularly at lower wavenumbers. This would allow examination of the metal-ligand bonds, and may allow identification of intermediates in the decomposition pathways of the precursors. The use of inert infrared windows instead of NaCl would reduce problems with adsorption of water, but these materials are considerably more expensive.

Finally, the addition of a purging "dome" around the mirrors, reactor and detector would reduce the influence of atmospheric carbon dioxide and water.

Surface spectroscopic methods, such as attenuated total reflectance (ATR) could also provide some insight into the film growth process. Integrating these methods into the CVD equipment would be somewhat more difficult than for the gas-phase infrared study.

REFERENCES

1. Seshan, K. *Handbook of Thin Film Deposition, Second Edition*; Noyes Publications: Norwich, NY, 2002.

2. Rappoli, B. J.; DeSisto, W. J. *Applied Physics Letters* **1996**, *68*(19), 2726-2728.

3. Hampden-Smith, J. M.; Kodas, T. T. *Chemistry of Metal CVD* VCH Publishers: New York, N. Y., 1994.

4. Gordon, R. G. ; Becker, J.; Hausmann, D.; Suh, S. *Chemistry of Materials* **2001**, *13*, 2463-2464.

5. Lau, K. K. S.; Lewis, H. G. P.; Limb, S. J.; Kwan, M. C.; Gleason, K. K. *Thin Solid Films* **2001**, *395*, 288-291.

6. Huppertz, H.; Engl, W. *IEEE Transactions on Electron Devices* **1979**, *26*(4), 658-662.

7. Adams, A. C.; Capio, C. D. *J. Electrochem. Soc.* **1979**, *126*(6), 1042-1046.

8. Levin, R. M.; Evans-Lutterodt, K. *Journal of Vacuum Science and Technology* **1983**, *B1*(1), 54-61.

9. Vogel, R. H.; Butler, S. R.; Feigl, F. J. *Journal of Electronic Materials* **1985**, *14*(3), 329-342.

10. Becker, F. S.; Pawlik, D.; Anzinger, H.; Spitzer, A. *Journal of Vacuum Science and Technology* **1987**, *B5*(6), 1555-1563.

11. Delprier, B. ; Vinante, C.; Morancho, R. *Journal of Analytical and Applied Pyrolysis* **1988**, *13*, 141-149.

12. Desu, S. B. *Journal of the American Ceramic Society* **1989**, *72*(9), 1615-1621.

13. Kalidindi, S. R.; Desu, S. B. *J. Electrochem. Soc.* **1990**, *137*(2), 624-628.

14. Sorita, T.; Shiga, S.; Ikuta, K.; Egashira, Y.; Komiyama, H. *J. Electrochem. Soc.* **1993**, *140*(10), 2952.

15. Kim, E. J.; Gill, W. N. *J. Electrochem. Soc.* **1995**, *142*(2), 676-682.

16. Senkevich, J. J.; Desu, S. B. *Chemical Vapor Deposition* **1998**, *4*(3), 92-94.

17. Merchant, T. P.; Gobbert, M. K.; Cale, T. S.; Brooks, L. J. *Thin Solid Films* **2000**, *365*, 368-375.

18. Labun, A. H. ; Moffat, H. K.; Cale, T. S. *Journal of Vacuum Science and Technology* **2000**, *B18*(1), 267-278.

19. Coltrin, M. E.; Ho, P.; Moffat, H. K.; Buss, R. J. *Thin Solid Films* **2000**, *365*, 251-263.

20. Nguyen, S.; Dobuzinsky, D.; Harmon, D.; Gleason, R.; Fridmann, S. *J. Electrochem. Soc.* **1990**, *137*(7), 2209-2215.

21. Kubo, A.; Homma, T.; Murao, Y. *J. Electrochem. Soc.* **1996**, *143*(5), 1769-1773.

22. Martin, J. G.; O'Neal, H. E.; Ring, M. A.; Roberts, D. A.; Hochberg, A. K. *J. Electrochem. Soc.* **1995**, *142*(11), 3873-3880.

23. Rand, M. J. *J. Electrochem. Soc.* **1973**, *120*(5), 686-693.

24. Goto, T.; Vargas, R.; Hirai, T. *Journal De Physique* **1993**, *3*(3), 297.

25. Vargas, R.; Goto, T.; Zhang, W.; Hirai, T. *Applied Physics Letters* **1994**, *65*(9), 1094-1096.

26. Arndt, J.; Klippe, L.; Stolle, R.; Wahl, G. *Journal De Physique IV* **1995**, *5*(C), 119-126.

27. Uemiya, S.; Kajiwara, M.; Kojima, T. *Ceramics Processing* **1997**, *43*(11A), 2715-2723.

28. Battison, G. A.; Gerbasi, R.; Porchia, M.; Gasparotto, A. *Chemical Vapor Deposition* **1999**, *5*(1), 13-20.

29. Malandrino, G.; Lo Nigro, R.; Fragala, I. L. *Chemical Vapor Deposition* **1999**, *5*(2), 59-61.

30. Montes de Oca, J. A.; Vargas, J. R.; Godinez, J. *Surface Engineering* **2000**, *16*(1), 66-69.

31. Igumenov, I. K.; Gelfond, N. V.; Galkin, P. S.; Morozova, N. B.; Fedotova, N. E.; Zharkova, G. I.; Shipachev, V. I.; Reznikova, E. F.; Ryabstev, A. D.; Kotsupalo, N. P.; Titarenko, V. I.; Dikov, Y. P.; Distler, V. V.; Buleev, M. I. *Desalination* **2001**, *136*, 273-280.

32. Gelfond, N. V.; Galkin, P. S.; Igumenov, I. K.; Morozova, N. B.; Fedotova, N. E.; Zharkova, G. I.; Shubin, Yu. V. *Journal De Physique IV* **2001**, *11*(Pr3), 593-599.

33. Morozova, N. B.; Zharkova, G. I.; Semyannikov, P. P.; Sysoev, I. K.; Igumenov, I. K.; Fedotova, N. E.; Gelfond, N. V. *Journal De Physique IV* **2001**, *11*(Pr3), 609-616.

34. Utriainen, M.; Kroger-Laukkanen, M.; Johansson, L.-S.; Niinisto, L. *Applied Surface Science* **2000**, *157*, 151-158.

35. Hierso, J.-C.; Feurer, R.; Klack, P. *Chemistry of Materials* **2000**, *12*, 390-399.

36. Erhardt, M. K.; Nuzzo, R. G. *Langmuir* **1999**, *15*, 2188-2193.

37. Stryckmans, O.; Segato, T.; Duvigneaud, P. H. *Thin Solid Films* **1996**, *283*, 17-25.

38. Chen, Y.; Kaesz, H. D. *Applied Physics Letters* **1988**, *53*(24), 1591-1592.

39. Xue, Z.; Strouse, M. J.; Shuh, D. K.; Knobler, C. B.; Kaesz, H. D.; Hicks, R. F.; Williams, R. S. *Journal of the American Chemical Society* **1989**, *111*, 8779-8784.

40. Kwon, J.-H.; Yoon, S.-G. *Thin Solid Films* **1997**, *303*, 136-142.

41. Choi, E.-S.; Park, C.-B.; Yoon, S.-G. *Chemical Vapor Deposition* **2001**, *7*(6), 260-264.

42. Kumar, R.; Roy, S.; Rashidi, M.; Puddephatt, R. J. *Polyhedron* **1989**, *8*(4), 551-553.

43. Watkins, J. J.; Blackburn, J. M.; McCarthy, T. J. *Chemistry of Materials* **1999**, *11*, 213-215.

44. Serp, Ph.; Hireso, J.-C.; Feurer, R.; Kihn, Y.; Klack, Ph.; Faria, J. L.; Aksoylu, A. E.; Pacheco, A. M. T.; Figueiredo, J. L. *Carbon* **1999**, *37*, 527-530.

45. Tagge, C. D.; Simpson, R. D.; Bergman, R. G.; Hostetler, M. J.; Girolami, G. S.; Nuzzo, R. G. *Journal of the American Chemical Society* **1996**, *118*, 2634-2643.

46. Houlton, D. J.; Jones, A. C.; Haycock, P. W.; Williams, E. W.; Bull, J.; Critchlow, G. W. *Chemical Vapor Deposition* **1995**, *1*(1), 26-28.

47. Veith, M.; Altherr, A.; Lecerf, N.; Mathur, S.; Valtchev, K.; Fritscher, E. *NanoStructured Materials* **1999**, *12*, 191-194.

48. Gu, S.; Atanasova, P.; Hampden-Smith, M. J.; Kodas, T. T. *Thin Solid Films* **1999**, *340*, 45-52.

49. Smith, R. C. ; Taylor, C. J.; Roberts, J.; Campbell, S. A.; Tiner, M.; Hegde, R.; Hobbs, C.; Gladfelter, W. L. *Chemistry of Materials* **2000**(12), 2822-2824.

50. Weiss, F.; Schmatz, U.; Pisch, A.; Felten, F.; Pignard, S.; Senateur, J. P.; Abrutis, A.; Frohlich, K.; Selbmann, D.; Klippe, L. *Journal of Alloys and Compounds* **1997**, *251*, 264-269.

51. Araki, T.; Yuasa, T.; Kurosaki, H.; Yamada, Y.; Hirabayashi, I.; Kato, T.; Hirayama, T.; Iijima, Y. S. T. *Superconductor Science and Technology* **2002**, *15*, L1-L3.

52. Veith, M.; Lecerf, N.; Mathur, S.; Shen, H.; Hufner, S. *Chemistry of Materials* **1999**, *11*, 3103-3112.

53. Daniele, S.; Bragato, C.; Battison, G. A.; Gerbasi, R. *Electrochemica Acta* **2001**, *46*, 2961-2966.

54. Chu, J. C. S.; Breslin, J.; Wang, N. S.; Lin, M. C. *Materials Letters* **1991**, *12*, 179-184.

55. Hanaoka, K.; Ohnishi, H.; Tachibana, K. *Japanese Journal of Applied Physics* **1993**, *32*(10), 4774-4778.

56. Momose, S.; Nakamura, T.; Tachibana, K. *Japanese Journal of Applied Physics* **2000**, *39*(9B), 5384-5388.

57. Clausen, S.; Bak, J. *J. Quant. Spectrosc. Radiat. Transfer* **1999**, *61*(2), 131-141.

58. Van Der Vis, M. G. M.; Konings, R. J. M.; Oskam, A.; Snoeck, T. L. *Journal of Molecular Structure* **1992**, *274*, 47-57.

59. Van Der Vis, M. G. M.; Cordfunke, E. H. P.; Konings, R. J. M. *Journal De Physique IV* **1993**, *C3*, 75-82.

60. Kawahara, T. ; Yuuki, A.; Yusuji, M. *Japanese Journal of Applied Physics* **1992**, *31*, 2925-2930.

61. Arno, J.; Yuan, Z.; Murphy, S. *J. Electrochem. Soc.* **1999**, *146*(1), 276-280.

62. Whidden, T. K.; Doiron, S.; Lee, S. Y. *Proceedings of the First International Symposium on Dielectric Materials for Advanced Electronic Packaging.*

63. Nakamoto, K. *Infrared Spectra of Inorganic and Coordination Compounds, 5th Edition*; Wiley: NY, 1997.

64. Barison, S.; Fabrizio, M.; Carta, G.; Rossetto, G.; Zanella, P.; Barreca, D.; Tondello, E. *Thin Solid Films* **2002**, *405*, 81-86.

BIOGRAPHY OF THE AUTHOR

Tyler Philip Martin was born in Boston, Massachusetts on September 25, 1977. He was raised in Hampden, Maine and graduated from Hampden Academy in 1996. He attended the University of Maine and graduated in 2000 with a Bachelor of Science degree in Chemical Engineering. That same year, he entered the Chemical Engineering graduate program at the University of Maine.

After receiving his degree, Tyler will be attending Massachusetts Institute of Technology to begin work towards a Doctor of Philosophy degree in Chemical Engineering. Tyler is a candidate for the Master of Science degree in Chemical Engineering from The University of Maine in August, 2002.